



# Progress in integrating remote sensing data and hydrologic modeling

Progress in Physical Geography

2014, Vol. 38(4) 464–498

© The Author(s) 2014

Reprints and permission:

sagepub.co.uk/journalsPermissions.nav

DOI: 10.1177/0309133314536583

ppg.sagepub.com



**Xiaoyong Xu**

University of Waterloo, Canada

**Jonathan Li**

University of Waterloo, Canada

**Bryan A. Tolson**

University of Waterloo, Canada

## Abstract

Remote sensing and hydrologic modeling are two key approaches to evaluate and predict hydrology and water resources. Remote sensing technologies, due to their ability to offer large-scale spatially distributed observations, have opened up new opportunities for the development of fully distributed hydrologic and land-surface models. In general, remote sensing data can be applied to land-surface and hydrologic modeling through three strategies: model inputs (basin information, boundary conditions, etc.), parameter estimation (model calibration), and state estimation (data assimilation). There has been an intensive global research effort to integrate remote sensing and land/hydrologic modeling over the past few decades. In particular, in recent years significant progress has been made in land/hydrologic remote sensing data assimilation. Hence there is a demand for an up-to-date review on these efforts. This paper presents an overview of research efforts to combine hydrologic/land models and remote sensing products (mainly including precipitation, surface soil moisture, snow cover, snow water equivalent, leaf area index, and evapotranspiration) over the past decade. This paper also discusses the major challenges remaining in this field, and recommends the directions for further research efforts.

## Keywords

data assimilation, evapotranspiration, land surface and hydrologic models, leaf index area, precipitation, remote sensing, snow cover, snow water equivalent, soil moisture

## 1 Introduction

Changes in the spatial and temporal patterns of water resources are expected to play a major role in driving the impacts of climate and global change on human settlements and infrastructure (Bates et al., 2008). The monitoring and prediction of water resources under climate change rely on in-situ and remote sensing observations,

and reliable hydrologic modeling systems. In-situ observations are generally based upon uneven point sources, and have limited and

---

### Corresponding author:

Xiaoyong Xu, University of Waterloo, 200 University Avenue West, Waterloo, Ontario, N2L 3G1, Canada.

Email: xiaoyong.xu@uwaterloo.ca

sparse spatial coverage except in developed areas. Remote sensing offers better geographical coverage and holds the capability to provide land/hydrologic models with extensive amounts of spatially distributed data. A variety of hydrologic variables can be estimated using remote sensing (see the review papers by Dietz et al., 2012; Li et al., 2009; Rango, 1994; Tang et al., 2009; Wang and Qu, 2009; Zheng and Moskal, 2009).

Remotely sensed hydrologic products have been increasingly available over the past decades, which has opened up new possibilities for advances in the integration of remote sensing and land surface/hydrologic models. A number of review papers on this topic have been published, but usually focused upon only soil moisture or snow products (e.g. Loumagne et al., 2001; Moradkhani, 2008; Wagner et al., 2009). A relatively comprehensive review of integrating remote sensing data and hydrologic modeling was provided by Kite and Pietroniro (1996). Since then, however, significant progress has been made in this area, especially due to advances in land/hydrologic data assimilation. Hence there is a demand for an up-to-date review on recent efforts in this field. This paper presents an overview of progress in combining remote sensing and hydrologic modeling over the last decade, with a focus on the development of satellite data assimilation. The aim is to provide the research community with a guide for future efforts. The remainder of the paper is organized as follows. Section II summarizes the key approaches that are used to integrate remote sensing data and land/hydrologic models. In section III, we review the integration of hydrologic/land-surface models with six categories of remotely sensed products (precipitation, surface soil moisture, snow covered area, snow water equivalent, leaf area index, and evapotranspiration) during the past 10 years. Finally, this paper discusses the problems and challenges remaining in this field (section IV), and recommends future research directions (section V).

## **II Strategies for integrating remote sensing data and hydrologic modeling**

In general, remote sensing information can contribute to land-surface and hydrologic modeling through three strategies. First, remote sensing products can be applied to model inputs. Historically, this type of application has been dominant in incorporating remote sensing and hydrologic models. Remote sensing can provide hydrologic models with the required basin information, such as a digital elevation model and land cover. Furthermore, remote sensing-derived hydrologic variables (e.g. satellite precipitation) can be used to drive hydrologic models. Remote sensing can offer large-scale spatially distributed data for forcing hydrologic models (e.g. Andersen et al., 2002; Stisen et al., 2008). However, the ‘forcing’ suffers considerably from uncertainties and biases in remote sensing measurements. Uncertainties associated with remote sensing-based forcing data may be enlarged during the model’s forward integration and therefore could significantly degrade the model performance. For instance, an uncertainty source from satellite-based precipitation products could exert a negative effect on the ensemble prediction of streamflow (Moradkhani et al., 2006). Collier (2009) demonstrated the propagation of uncertainty in radar-based rainfall input in hydrologic modeling and the associated impact on flow simulations.

The second strategy is its application to parameter estimation. Hydrologic models typically contain substantial conceptual, effective parameters that are hard or impractical to directly measure. These parameters need to be calibrated to the best-fitting local values so that an optimal agreement between the modeled and observed variables can be obtained. Salvucci and Entekhabi (2011) demonstrated that AMSR-E (Advanced Microwave Scanning Radiometer for EOS) soil moisture product was useful for the calibration of the soil

hydraulic properties in the Noah land surface model (LSM). Parajka et al. (2006, 2009) showed that a multi-objective calibration of a hydrologic model with SCAT (Scatterometer on European Remote Sensing Satellite) derived soil moisture information enhanced the soil moisture simulations in both gauged and ungauged catchments.

The third strategy is its application to state estimation. A state estimation problem is also referred to as data assimilation, which is a process to constrain the model simulations with observations to improve estimation of the state variable. A great number of methods have been developed for land/hydrologic data assimilation (Table 1). A simplistic method is a direct insertion, which uses an observed variable value to directly replace the simulated equivalent at each observation time (Figure 1a). The method imposes an observation as the sole strong constraint regardless of its quality. If the model provides a good estimate, it would not be reasonable to replace it with a poor-quality observation. To this end, advanced data assimilation schemes update the model simulations through an optimal constraint that is based upon the estimated measurement and model forecast errors (Figure 1, b and c).

Data assimilation technologies are being increasingly used in a great variety of disciplines for incorporating observations into models. Data assimilation methods and their application to land surface and hydrologic modeling have been recently reviewed by some researchers (e.g. Liu and Gupta, 2007; Y. Liu et al., 2012; Reichle, 2008; Vereecken et al., 2008). The reader is referred to these articles for details on the properties of different algorithms (e.g. error covariance calculation and evolution, computational demands). Here we briefly describe two categories of state estimation problems: smoothing (Figure 1b) and filtering (Figure 1c), which involve the most commonly used advanced methods for hydrologic data assimilation. The basic idea of a 'smoothing' assimilation is to seek

an optimal fit of the model state to observations over a time window, which is achieved either by a maximum-likelihood estimator (e.g. a four-dimensional variational method, 4DVAR) or by a variance minimizing estimator (e.g. an ensemble Kalman smoother, EnKS). The former assumes that the error statistics of the background (a priori state) and the observation are known (e.g. Gaussian), and the state with the maximum likelihood is sought by minimizing a cost function that measures the distance of the model state (unknown) to the observations and to the background. Specifically, (1) run the model with the first-guess estimate of initial and boundary conditions to obtain model output results over the time window; (2) calculate the cost function and determine whether it is small enough (i.e. whether the minimization convergence criterion is met); (3) if not, adjust the initial or boundary conditions based upon a descent direction, which is determined by the gradient of the cost function; and (4) repeat the above steps until the convergence criterion is met. On the other hand, a variance minimizing estimator directly derives the analysis state based upon an analysis equation, which can ensure that the total analysis error variances are minimum over the whole space and time domain. The two estimators are identical when the system is linear (van Leeuwen and Evensen, 1996). In a smoothing assimilation the state estimation over the assimilation interval (time window) is influenced by all the observations distributed in this time interval (Figure 1b), i.e. the observational information is propagated not only from the past into the future but also from the future into the past.

In contrast, a 'filtering' adjusts only the current state. A 'filtering' algorithm sequentially conducts a forecast step and an analysis step. In the forecast step, the forecast model is integrated forward in time, while at the analysis step new observation is used to adjust the current

**Table 1.** Summary of land/hydrologic data assimilation methods.

Methods	Specifications	Examples
Direct insertion	Directly replace the model forecast with an observation.	Rodell and Houser (2004); Tang and Lettenmaier (2010)
Statistical correction	Statistical characteristics (e.g. mean, standard deviation) of the modeled variables are adjusted to match those observed.	Houser et al. (1998); Pauwels et al. (2002)
Successive corrections	Update the modeled variables at each grid based on the surrounding observations by multiple passes. The weight of an observation depends upon its distance to the model grid.	Rodríguez et al. (2003)
Nudging	Add a nudging term, which is proportional to the model/observation difference, to the prognostic equations. The nudging term will force the integration of prognostic equations towards observations.	Brocca et al. (2010); Houser et al. (1998)
Optimal interpolation	Observations are weighted according to known or estimated errors. Determine the optimum weight (gain) matrix using least squares so that the total analysis error is minimum.	Houser et al. (1998); Liston and Hiemstra (2008)
Three-dimensional variational (3DVAR)	Seek a state with the maximum likelihood by iteratively minimizing a cost function, which measures the misfit between the model simulations and observations. Dynamical constraints are included when minimizing the cost function.	Seo et al. (2003a, 2003b)
Four-dimensional variational (4DVAR)	Extension of 3DVAR to the time dimension. A smoothing algorithm. Seek an optimal fit of the model forecast to observations over an assimilation interval. The state estimation is affected by all the observations within the assimilation interval.	Reichle et al. (2001a, 2001b)
Kalman Filter (KF)	A variance minimizing analysis in the framework of a sequential assimilation. Each assimilation cycle consists of two steps: the forecast step (the model state is integrated forward in time) and the analysis step (the model prediction is updated with observations). Explicit error covariance propagation. Valid only for linear systems.	Crow and Zhan (2007); Crow et al. (2005); Walker and Houser (2001)

(continued)

**Table 1.** (continued)

Methods	Specifications	Examples
Extended Kalman Filter (EKF)	A non-linear counterpart of the KF. A linearized and approximate error covariance is used. Able to deal with some non-linear/Gaussian processes.	Dong et al. (2007); Draper et al. (2009); Francois et al. (2003); Sun et al. (2004)
Ensemble Kalman Filter (EnKF)	A Monte Carlo variant of the KF. The error statistics are represented by an ensemble of model states and the ensemble spread defines the error variance. The ensemble mean is the best estimate (assumption of Gaussian statistics).	Crow and Wood (2003); De Lannoy et al. (2010, 2012); Draper et al. (2012); Reichle et al. (2002, 2007); Su et al. (2008, 2010)
Ensemble Kalman Smoother (EnKS)	Similar to EnKF except that the time dimension is included. A smoothing variance-minimizing estimator.	Crow and Ryu (2009)
Bayesian Filter	Seeks a posterior probability density function (PDF) at a current time given all the observations up to the current time based on Bayes theorem.	Kolberg et al. (2006)
Particle Filter (PF)	A Monte Carlo importance sampling is used, and the posterior PDF of the model state is represented by a weighted sum of the particles that are sampled from a proposal distribution. Update the importance weights at the analysis step. A non-linear/non-Gaussian filter.	Dechant and Moradkhani (2011); Moradkhani et al. (2006, 2012)

model state. Starting with the updated state estimation, the model is then integrated forward to the next observation time. Therefore, the observational information is propagated in a sequential manner (Figure 1c). A ‘filtering’ estimation can be accomplished with a maximum-likelihood estimator (e.g. a three-dimensional variational method, 3DVAR), a variance minimizing estimator (e.g. the Kalman filter, KF; the extended Kalman filter, EKF; and the ensemble Kalman filter, EnKF), or a recursive Bayesian filter (e.g. the particle filter, PF).

In practice, land/hydrologic forecasting is often difficult since the hydrology and Earth system contains various complex, non-linear stochastic processes. A subtle uncertainty source arising from model inputs or parameters may lead to substantial forecast biases. A state

estimation via a sequential assimilation or a strong-constraint 4DVAR largely deals with the uncertainties in the model input fields, and ignores deficiencies in the model physics and parameters (i.e. assuming that the model is perfect). In contrast, a parameter estimation handles uncertain model parameters, but cannot account for deficiencies associated with model inputs. Hence, to obtain the desired outcomes, some researchers proposed to simultaneously update the model state and parameters, e.g. the augmentation method (Gillijns and De Moor, 2007; Yang and Delsole, 2009) and the dual state-parameter estimation method (Moradkhani et al., 2005), although this type of application has not yet been effectively exploited for remote sensing data. A main obstacle is the dynamic instability problem due to the interactions between the model

state variables and parameters as well as their inconsistent adjustment speeds (Liu and Gupta, 2007; Yang and Delsole, 2009).

### III Integration of remote sensing data with hydrologic and land-surface models

There has been an intensive global research effort to integrate remote sensing data and hydrologic modeling over the past decade. The relevant work is largely focused on remote sensing-based precipitation, surface soil moisture, snow cover, snow water equivalent, leaf area index, and evapotranspiration.

#### I Precipitation

Precipitation plays a dominant role in the Earth's water and energy cycles, and is the most important forcing variable of hydrologic models. Historically, a rain gauge network has been the main observing system providing precipitation data for hydrologic applications. Due to being based upon uneven point sources, however, the spatial coverage of rain gauge observations is usually limited, especially in developing regions. When there is a large spatial variability in precipitation system (e.g. mesoscale and microscale intense convective storms), gauge-based precipitation may contain substantial sampling errors and uncertainties. Satellite-based remote sensing, which can overcome the limitation of rain gauge observations in spatial coverage, provides a useful tool for estimating precipitation on a large scale, especially in ungauged basins. Satellite technologies using visible/near-infrared, passive microwave, and active radar sensors (Table 2) have been developed for estimating precipitation (e.g. Kidder and Vonder Haar, 1995; Kummerow et al., 1996; Stephens and Kummerow, 2007). Satellite precipitation has been an important source to force hydrologic models. For example, precipitation estimates from

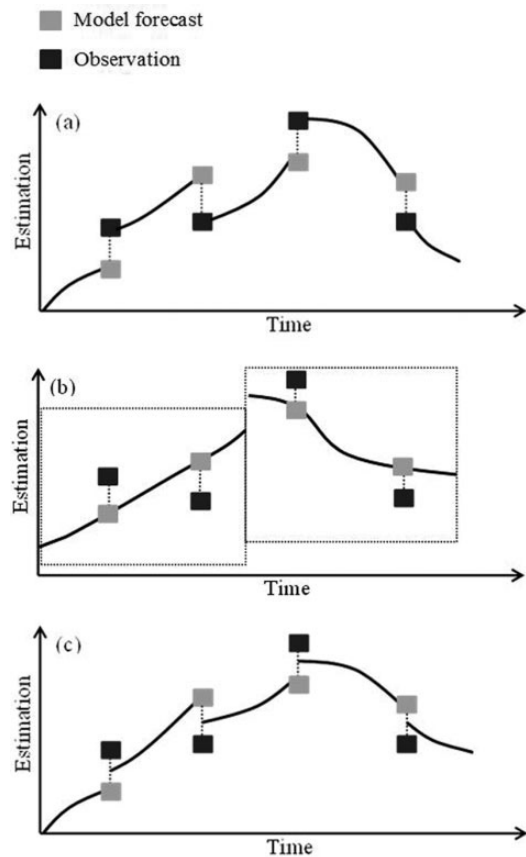


**Figure 1.** Schematic of different strategies for hydrologic data assimilation: (a) direct insertion; (b) smoothing; (c) filtering.

Source: Adapted from Reichle (2008) and Dorigo et al. (2007).

geostationary Meteorological Satellites (METEOSAT) thermal infrared data were applied to force the distributed hydrologic model MIKE SHE code for runoff modeling in the Senegal River basin (Andersen et al., 2002; Stisen and Sandholt, 2010; Stisen et al., 2008). Grimes and Diop (2003) used METEOSAT thermal infrared imagery-derived precipitation to drive a lumped hydrologic modeling for the Qualia catchment. More recently, T. Liu et al. (2012) presented the use of the Chinese meteorological satellite Fengyun-2C precipitation in modeling the China's Tarim River basin runoff with MIKE SHE.

**Table 2.** Summary of remote sensing techniques for precipitation estimation.

Sensors	Retrieval methods	Pros	Cons
Visible/infrared (IR) (e.g. from GOES, METEOSAT, GMS)	Rain rate is estimated based upon the cloud top temperatures	Good spatial and temporal resolution	Weak physical connection to precipitation
Spaceborne passive microwave sensors (e.g. SSM/I, TMI, AMSU-B)	A Bayesian approach to match the observed brightness temperatures $T_b$ with those from simulated hydrometeor profiles (Imagers); a combination of $T_b$ at different frequencies (Sounders)	Better physical connection to precipitation	Coarse spatial and temporal resolution
Spaceborne radar (e.g. PR on TRMM)	Radar reflectivity ( $Z$ )-rain rate ( $R$ ) and specific attenuation ( $k$ )-radar reflectivity ( $Z$ ) relations	Direct measurement of the three-dimensional structure of precipitation	The variability of the drop size distributions (DSDs) strongly affects precipitation estimation
Ground-based radar (e.g. WSR-88D)	Radar reflectivity ( $Z$ )-rainfall rate ( $R$ ) relationship	High spatial and temporal resolution	Limited radar coverage in mountainous regions; brightband contamination

Abbreviations: GOES, geostationary operational environmental satellite; METEOSAT, Meteorological Satellites; GMS, Japan's Geostationary Meteorological Satellite; SSM/I, Special Sensor Microwave/Imager; TMI, Tropical Rainfall Measuring Mission (TRMM) Microwave Imager; AMSU-B, Advanced Microwave Sounding Unit-B; PR, Precipitation Radar on TRMM WSR-88D, the US NEXRAD Weather Surveillance Radar-1988 Doppler.

Kalinga and Gan (2010) examined the use of the combined infrared and microwave satellite rainfall data in the SACramento Soil Moisture Accounting (SAC-SMA) model that is a conceptual rainfall-runoff model. The rainfall products were derived from the infrared data collected by the Tropical Rainfall Measuring Mission (TRMM) satellite and geostationary operational environmental satellite (GOES), which were then adjusted with the TRMM Microwave Imager (TMI) data. Although satellite remote sensing can provide large-scale spatially distributed rainfall data, significant improvements in runoff simulations were not guaranteed when satellite precipitation data, in comparison to rain gauge observations, were used (e.g. Andersen et al., 2002). This is probably related to uncertainties in satellite-based precipitation products (Moradkhani et al., 2006; Stisen and Sandholt, 2010). For example,

sensors onboard polar-orbiting satellites usually have relatively coarse temporal sampling frequency (1–2 visits per day), which will affect their ability to accurately estimate a high spatio-temporal variability (e.g. diurnal characteristics) of precipitation. The merged satellite visible/near-infrared and microwave rainfall estimates contain less significant uncertainties and could lead to better streamflow simulations than single-sensor precipitation.

Ground-based weather radars (Table 2) provide another efficient remote sensing tool for measuring rainfall. The radar-based quantitative precipitation estimation (QPE) relies on a radar reflectivity ( $Z$ ) to rainfall rate ( $R$ ) relationship. The  $Z$ – $R$  relationship varies with the rainfall systems. Applying different  $Z$ – $R$  relationships based on precipitation echo classification can improve the accuracy of radar rainfall estimation (Xu et al., 2008; Zhang et al., 2011). The

introduction of radar-based rainfall data into hydrologic models has been demonstrated to be useful for the simulations of streamflow, flood events and water budgets (e.g. Guo et al., 2004; Safari and De Smedt, 2008; Yang et al., 2004). Currently, ground-based radars, e.g. the US Next Generation Radar (NEXRAD) Weather Surveillance Radar-1988 Doppler (WSR-88D), can provide high spatial (2 km in range by 1 deg in azimuth up to 4 km × 4 km) and temporal resolution (~6 min) QPE. Butts et al. (2005) reported the use of rainfall data (hourly and 4 km in space) observed by NEXRAD in a flexible hydrologic modeling system that originates from MIKE SHE. Results indicated that hydrologic prediction could benefit from the forcing of NEXRAD rainfall data. Traditionally, hydrologic modeling forced by radar-based rainfall inputs has generally been limited to small catchments ( $\leq 10,000 \text{ km}^2$ ) due to a limited detection coverage of a single radar (e.g. Butts et al., 2005; Cole and Moore, 2008). The deployment of the radar network (e.g. in the USA and Canada) has made it possible to conduct a high time and space resolution precipitation analysis for large regions (e.g. Zhang et al., 2011). Kitzmiller et al. (2011) indicated that QPE from multiple NEXRAD mosaic could be useful for streamflow simulations at large scales. In Europe, He et al. (2011) used QPE from a combination of five C-band Doppler radars to force a hydrologic model that was applied to the Skjern River catchment.

Radar rainfall estimates suffer from several known sources of uncertainty such as reflectivity calibration differences, inappropriate  $Z-R$  relationships, range degradation, and brightband contamination, which may affect rainfall-runoff modeling (e.g. Borga, 2002; Collier, 2009; Habib et al., 2008a, 2008b). A series of studies have been conducted to address how to mitigate the effects of uncertainty in radar rainfall estimates on hydrologic modeling. An automated  $Z-R$  selection and a brightband identification could improve radar rainfall estimation and therefore

flow simulations (Kitzmiller et al., 2011). Some efforts investigated the impact of gauge, radar, and gauge-adjusted radar rainfall forcings on runoff modeling, suggesting that a gauge-radar merged precipitation field generally led to optimal runoff simulations and prediction (e.g. Biggs and Atkinson, 2011; Cole and Moore, 2008, 2009; Kitzmiller et al., 2011; Sun et al., 2000). Germann et al. (2009) showed that the use of an ensemble of radar precipitation fields in a hydrologic model could improve flash flood simulation, especially in mountainous regions that often witness large uncertainty in radar precipitation estimation.

Advanced data assimilation schemes estimate observational errors and minimize their impact on model simulations. The basic idea of data assimilation is to merge observations into the framework of dynamic models by measuring the model and measurement uncertainties. Precipitation observations usually cannot be assimilated into a hydrologic model system (standalone) because the precipitation field is not a state variable. In a coupled atmospheric-land/hydrologic model system the assimilation of satellite or radar precipitation is applicable. Seo et al. (2003b) reported a real-time variational assimilation of radar precipitation in the Hydrology Laboratory-Research Distributed Hydrologic Model (HL-RDHM). Their work demonstrated that the updating of model state variables with radar rainfall and other observations improved streamflow modeling.

## 2 Surface soil moisture

Soil moisture is an important variable for numerical weather, climate, and hydrologic forecasts. This is because soil moisture plays a crucial role in the hydrologic cycle by controlling the partitioning of water and energy fluxes at the land surface and the moisture exchanges at the soil-vegetation-atmosphere interface. Surface soil moisture can be estimated using various remote sensing instruments including microwave,

optical, and thermal infrared sensors (e.g. Wang and Qu, 2009). Microwave techniques are of particular value for surface soil moisture estimation because microwave measurements are sensitive to changes in the soil dielectric properties, which are strongly controlled by soil water content. Liquid water has a very high dielectric constant ( $\sim 80\text{--}90$  at  $0\text{--}20^\circ\text{C}$ ) while the dielectric constant is very low (only  $\sim 4$ ) for dry soil. Such a high contrast between the dielectric constants of wet and dry soils forms the basis for deriving soil moisture information from microwave remote sensing data. Both passive and active technologies have been developed for microwave estimation of surface soil moisture (Jackson, 2005). Over the past decades, the dominant spaceborne passive microwave sensor systems for soil moisture estimation include the Special Sensor Microwave Imager (SSM/I) (e.g. Jackson, 1997), the Scanning Multichannel Microwave Radiometer (SMMR) (e.g. Reichle and Koster, 2005), TMI (e.g. Bindlish et al., 2003), AMSR-E on the Aqua satellite (e.g. Njoku et al., 2003; Reichle et al., 2007), the European Space Agency (ESA) Soil Moisture and Ocean Salinity (SMOS) satellite (Kerr et al., 2012) that carries a novel instrument called Microwave Imaging Radiometer with Aperture Synthesis (MIRAS), and the newly launched Advanced Microwave Scanning Radiometer 2 (AMSR2). For spaceborne active measurements, the ESA Remote Sensing Satellite (ERS) Synthetic Aperture Radar (SAR) and Scatterometer (SCAT), the Canadian RADARSAT series (e.g. Merzouki et al., 2011), and the Advanced Scatterometer (ASCAT), successor of the SCAT, onboard the Meteorological Operational (Metop) satellite (e.g. Albergel et al., 2009; Bartalis et al., 2007) have been the main observing systems. Tables 3a and 3b provide the specifications for these passive and active microwave sensors, respectively. There is usually an inverse relationship between a sensor's temporal frequency and spatial resolution. The active SAR technology is able to scan the land at a high spatial resolution,

but the revisit time is very long. Passive microwave sensors onboard polar-orbiting satellites offer a higher time resolution (revisit per 1–3 days) due to their wide swaths, but generally result in relatively coarse spatial samplings.

Microwave sensors measure only the soil moisture within a near-surface layer. The soil thickness measured increases with the wavelength (approximately several tenths of the wavelength). For bare soil, the penetration depth is about 3–5 cm for L-band (1–2 GHz) sensors (e.g. SMOS), and only  $\sim 1\text{--}1.5$  cm for C (4–8 GHz) or X (8–12 GHz) band measurements (e.g. AMSR-E). Soil moisture estimation using microwave sensors is subject to vegetation effects. Where there is a vegetation cover, the radiation emitted or backscattered from the soil will be attenuated owing to the scattering and absorption by the vegetation canopy. The magnitude of the vegetation attenuation increases with the sensor frequency and the vegetation density. Hence soil moisture retrieval at high microwave frequencies ( $>5\text{--}6$  GHz) is valid only for bare soil or sparsely vegetated regions. Vegetation cover impacts upon sensors operating at low frequencies are less pronounced because the latter can penetrate moderately dense canopies. For example, L-band sensors (e.g. SMOS) can provide reliable measurements over a wide range of vegetation cover (biomass  $\leq 5\text{ kg/m}^2$ ). Overall, soil moisture retrieval is challenging for active microwave sensors because the radar signal is highly sensitive to local features of the soil surface (surface roughness, topography, vegetation, etc.), while passive microwave soil moisture products are usually more reliable due to higher signal-to-noise ratio and mature retrieval algorithms.

In hydrologic/land surface models, the calculation and simulation of soil water content is based upon an energy and water balance method. In general, the soil thermal and moisture regimes are resolved using multiple soil layers. There has been an intensive global research effort to

**Table 3a.** Summary of spaceborne passive microwave sensors for soil moisture estimation.

Sensor (satellite)	Period of operation	Frequency/footprint size (along track × cross track)	Polarization	Data acquisition
SMMR (Nimbus-7)	1978–1987	6.6 GHz / 148 km × 95 km 10.7 GHz / 91 km × 59 km 18.0 GHz / 55 km × 41 km 21.0 GHz / 50 km × 38 km 37.0 GHz / 27 km × 18 km	H & V	Every other day
SSM/I (DMSP)	1987–present	19.3 GHz / 69 km × 43 km 22.0 GHz / 60 km × 40 km 37.0 GHz / 37 km × 29 km 85.5 GHz / 15 km × 13 km	H & V	Daily
TMI (TRMM)	1997–present	10.7 GHz / 63 km × 39 km 19.4 GHz / 30 km × 18 km 21.3 GHz / 28 km × 28 km 37.0 GHz / 16 km × 10 km 85.5 GHz / 7 km × 5.1 km	H & V	Daily
AMSR-E (Aqua)	2002–2011	6.9 GHz / 74 km × 43 km 10.7 GHz / 51 km × 30 km 18.7 GHz / 27 km × 16 km 23.8 GHz / 31 km × 18 km 36.5 GHz / 14 km × 8 km 89.0 GHz / 6 km × 4 km	H & V	Daily
AMSR2 (GCOM-W1)	2012–present	6.9/7.3 GHz / 62 km × 35 km 10.7 GHz / 42 km × 24 km 18.7 GHz / 22 km × 14 km 23.8 GHz / 26 km × 15 km 36.5 GHz / 12 km × 7 km 89.0 GHz / 5 km × 3 km	H & V	Daily
MIRAS (SMOS)	2010–present	1.4 GHz / ~43 km × 43 km	H & V	Every 1–3 days

Abbreviations: SMMR, Scanning Multichannel Microwave Radiometer; SSM/I, Special Sensor Microwave/Imager; DMSP, Defense Meteorological Satellite Program; TMI, Tropical Rainfall Measuring Mission (TRMM) Microwave Imager; AMSR-E, Advanced Microwave Scanning Radiometer for EOS; AMSR2, Advanced Microwave Scanning Radiometer 2; GCOM-W1, Global Change Observation Mission 1st – Water ‘SHIZUKU’; MIRAS, Microwave Imaging Radiometer with Aperture Synthesis; SMOS, Soil Moisture and Ocean Salinity satellite.

integrate microwave soil moisture information and land surface/hydrologic modeling over the past decade. In particular, the assimilation of microwave measurements in land/hydrologic models has received considerable attention (Table 4). Some efforts focused upon a direct assimilation of microwave brightness temperature observations in land surface models to estimate soil moisture. A series of synthetic studies based upon the 1997 Southern Great Plains (SGP97) hydrology experiment demonstrated

that a direct assimilation of microwave brightness temperature data in land surface models could provide reliable soil moisture estimation (e.g. Reichle et al., 2001a, 2001b, 2002). In realistic situations, Margulis et al. (2002) used the EnKF method to assimilate airborne Electronically Steered Thinned Array Radiometer (ESTAR) 1.4 GHz surface brightness temperature measurements during SGP97 into the Noah LSM. Crow and Wood (2003) conducted similar assimilation experiments with the

**Table 3b.** Summary of spaceborne active microwave sensors for soil moisture estimation.

Sensor/satellite	Period of operation	Frequency	Polarization	Spatial resolution	Repeat cycle
SAR/ERS-1	1991–1999	5.3 GHz	VV	30 m	35 days
SAR/ERS-2	1995–2011	5.3 GHz	VV	25 m	35 days
ASAR/Envisat	2002–2012	5.3 GHz	VV/HH, HV/HH, VH/VV	30–1000 m	35 days
SAR/TerraSAR-X	2007–present	9.6 GHz	HH, VV, HV, VH	1–18 m	11 days
SAR/RADARSAT-1	1995–present	5.3 GHz	HH	8–100 m	24 days
SAR/RADARSAT-2	2007–present	5.4 GHz	HH, VV, HV, VH	3–100 m	24 days
SAR/JERS-1	1992–1998	1.3 GHz	HH	18 m	44 days
PALSAR/ALOS	2006–present	1.3 GHz	HH, VV, HV, VH	7–100 m	46 days
SCAT/ERS-1&2	1991–2011	5.3 GHz	VV	25 km/50 km	3–4 days
ASCAT/Metop	2006–present	5.3 GHz	VV	25 km/50 km	1–2 days

Abbreviations: ERS, European Remote Sensing Satellite; SAR, Synthetic Aperture Radar; ASAR, Advanced Synthetic Aperture Radar; Envisat, Environmental Satellite; JERS, Japanese Earth Resources Satellite; PALSAR, Phased Array type L-band Synthetic Aperture Radar; ALOS, Advanced Land Observing Satellite; SCAT, Scatterometer; ASCAT, the Advanced Scatterometer.

TOPMODEL-Based Land Surface-Atmosphere Transfer Scheme (TOPLATS) model. Their results showed that the assimilation of ESTAR brightness temperature measurements led to good soil moisture estimation not only in the surface layer but also in the root zone. Mattia et al. (2009) demonstrated that high spatial resolution surface soil moisture could be estimated through an integration of SAR data and hydrologic modeling with a constrained minimization technique. In their SAR retrieval algorithm, the hydrologic model provided the background information about soil moisture at coarse spatial resolution based on the Antecedent Precipitation Index (API) approach.

A great number of studies attempted to improve soil moisture simulations in land models through the assimilation of microwave soil moisture retrievals (i.e. soil moisture was retrieved from microwave brightness temperatures prior to data assimilation). As one of the pioneer studies, for instance, Houser et al. (1998) incorporated soil moisture derived from the NASA L-band (1–2 GHz) push broom microwave radiometer (PBM) mounted on a NASA C-130 aircraft into the hydrologic model TOPLATS with several assimilation schemes.

Results showed that all the assimilation schemes could produce substantial improvement in surface soil moisture simulations. Several studies (Ni-Meister et al., 2006; Reichle and Koster, 2005; Reichle et al., 2007) assimilated global surface soil moisture retrievals from SMMR and AMSR-E into the NASA Catchment LSM using the EnKF method. An improvement in the simulated surface soil moisture in terms of annual cycles and anomalies demonstrated the potential of a sequential assimilation of passive microwave remote sensing information to monitor surface soil moisture. In Draper et al. (2009), the EKF method was applied to assimilate AMSR-E near-surface soil moisture into the Interactions between Surface, Biosphere, and Atmosphere (ISBA) land model. The assimilation resulted in an efficient updating of root-zone soil moisture. More recently, multi-year near-surface soil moisture observations by AMSR-E and ASCAT were assimilated, separately or jointly, into the Catchment LSM with the EnKF technique (Draper et al., 2012). The study showed that the soil moisture simulations could be improved through the assimilation of either AMSR-E or ASCAT soil moisture products. A joint

**Table 4.** Summary of efforts to assimilate microwave soil moisture data into land/hydrologic models.

Authors	Microwave data	Data period	Land/hydrologic models	Assimilation methods	Study region
Reichle et al. (2001a, 2001b, 2002)	Simulated L-band brightness temperatures based upon SGP97	June to July 1997	A soil-vegetation-atmosphere transfer scheme (SVAT)	4D-VAR; EnKF	Central Oklahoma
Crosson et al. (2002)	Brightness temperatures by a ground-based SLMR during SGP97	23 June to 16 July 1997	A land surface flux-soil moisture model SHEELS	KF	Central Oklahoma
Crow and Wood (2003); Margulis et al. (2002)	Brightness temperatures by Airborne ESTAR during SGP97 (resolution: 800 m)	16 of the 30 days (18 June to 17 July 1997)	Noah LSM; TOPLATS model	EnKF (updating with both point- and footprint-scale observations)	Central Oklahoma
Merlin et al. (2006)	Synthetic SMOS-type soil moisture data		A distributed SVAT model	EnKF	The Walnut Gulch Watershed, Arizona
Pauwels et al. (2002)	Soil moisture retrievals from SAR on ERS-1 and 2 (resolution: 25–30 m)	13 measurements between October 1995 and February 2000	TOPLATS	Statistical correction	The Zwalm catchment, Belgium
Francois et al. (2003)	Soil moisture retrievals from SAR on ERS-1 (spatial resolution: 30 m)	25 measurements between 1995 and 1997	The two-layer conceptual hydrological model GRKAL	EKF	The Orgeval agricultural river basin, France
Ni-Meister et al. (2006); Reichle and Koster (2005)	SMMR (C-band) surface soil moisture retrievals (resolution: ~120 km)	January 1979 to August 1987	Catchment LSM	EnKF	Global; Eurasian catchments
Reichle et al. (2007)	Soil moisture retrievals from AMSR-E (X-band) and SMMR (C-band)	June 2002 to May 2006 (AMSR-E); January 1979 to August 1987 (SMMR)	Catchment LSM	EnKF	Global

(continued)

**Table 4.** (continued)

Authors	Microwave data	Data period	Land/hydrologic models	Assimilation methods	Study region
Draper et al. (2009)	Surface soil moisture retrievals from AMSR-E C-band observations (resolution: ~ 60 km)	Over 2006	The Interactions between Surface, Biosphere, and Atmosphere (ISBA) LSM	EKF	European domain
Li et al. (2012)	AMSR-E (X-band) soil moisture product (resampled spatial resolution: ~25 km)	2006–2007	Noah LSM	EnKF	The Little Washita watershed, Oklahoma
Brocca et al. (2010)	Soil wetness index (SWI) product from ASCAT (spatial resolution: 25 km)	January 2007 to June 2009	A rainfall-runoff model MISDc	Update the modeled saturation degree using a nudging scheme	5 subcatchments of the Upper Tiber River in central Italy
Draper et al. (2012)	Surface soil moisture retrievals from AMSR-E (X-band) and ASCAT	January 2007 to May 2010	Catchment LSM	EnKF	CONUS and southeast Australia
Crow et al. (2005)	Soil moisture retrievals from TMI X-band observations	December 1997 to September 2002	An antecedent precipitation index (API) model	Updating API based upon TMI soil moisture with the KF	26 basins in the US Southern Great Plains
Crow and Zhan (2007)	Soil moisture retrievals from dual- and single-polarization AMSR-E X-band brightness temperatures, ERS-1 and -2 SCAT backscattering coefficients, and GOES thermal observations, respectively	1 July 2002 to 31 December 2005 (AMSR-E); 1 January 1997 to 31 December 2005 (SCAT); 2002–2004 growing seasons (GOES)	API model	Rainfall correction based upon remotely sensed soil moisture with the KF	CONUS
Crow et al. (2009)	AMSR-E (X-band) soil moisture retrievals	1 July 2002 to 31 December 2006	API model	Rainfall correction with the KF	CONUS
Crow and Ryu (2009)	Synthetic remotely sensed soil moisture retrievals by the SAC model		The Sacramento (SAC) hydrologic model	Simultaneously adjust the model state (EnKF or EnKS) and rainfall accumulations (KF)	MOPEX basins, USA

Abbreviations: KF, Kalman Filter; EKF, Extended Kalman Filter; EnKF, Ensemble Kalman Filter; EnKS, Ensemble Kalman Filter; SLMR, S- and L-band Microwave Radiometer; TOPLATS, TOPMODEL-based land atmosphere transfer scheme; MOPEX, Model Parameterization Experiment.

assimilation of two sensor products led to the best soil moisture estimation.

During a flooding event, the affected areas are usually characterized by wet pre-storm soil moisture conditions (i.e. low microwave brightness temperatures). This provides an opportunity for improving streamflow forecasts by using microwave remote sensing observations to identify antecedent soil moisture conditions. Jacobs et al. (2003) introduced the surface soil moisture observed by ESTAR during the SGP97 hydrology experiment into a lumped rainfall-runoff model. The ESTAR soil moisture retrievals were applied to represent antecedent soil moisture conditions and to update the curve numbers and the runoff predictions based upon a strong correlation between the curve number and soil moisture in the Soil Conservation Service (SCS) curve number method. Results showed an enhancement in runoff forecasts for the watersheds at different spatial scales. Bindlish et al. (2009) used AMSR-E brightness temperatures at two bands (6.9 GHz and 10.7 GHz) as inputs to a statistical adaptive model, and enhanced streamflow simulations. Pauwels et al. (2002) improved the simulated hydrographs in TOPLATS through the assimilation of ERS SAR soil moisture estimates using a statistical correction approach. Similarly, an EKF method was applied to assimilate soil moisture retrieved from ERS-1 SAR data into a lumped rainfall-runoff model coupled with a land surface scheme (Francois et al., 2003). The study demonstrated that the sequential assimilation of SAR data had the potential to improve hydrologic runoff simulations by quantifying uncertainties in the model's forcing data. Regarding the earlier studies of assimilating ERS SAR soil moisture retrievals into hydrologic models, we refer the readers to a review paper by Loumagne et al. (2001).

Crow et al. (2005) suggested that the predictive capability of land surface's response to precipitation was enhanced when TMI-derived surface soil moisture was sequentially

assimilated into an API model. Brocca et al. (2010) explored the impact on flood forecasting of assimilating an ASCAT-based soil wetness index in a rainfall-runoff model. Results revealed that the assimilation of the ASCAT soil moisture estimates via a simple nudging scheme led to an enhancement in runoff prediction, in particular when the initial soil wetness conditions are undetermined.

The aforementioned efforts have demonstrated that the adjusting and constraint of pre-storm soil moisture conditions in hydrologic models with remotely sensed soil moisture could improve the characterization of antecedent soil moisture conditions and therefore the prediction of runoff response to subsequent rainfall. Crow and Ryu (2009) proposed a new assimilation scheme in which remotely sensed surface soil moisture measurements were employed to simultaneously adjust both antecedent soil moisture and rainfall accumulations during hydrologic modeling. Their work was motivated by the additional capability of soil moisture data to filter errors contained in satellite-based rainfall products (Crow and Zhan, 2007; Crow et al., 2009). Preliminary results indicated that the new approach outperformed those schemes which considered only the calibration of antecedent wetness conditions.

Until recently, X- and C-band spaceborne microwave observations were dominant for surface soil moisture assimilation. As mentioned before, soil moisture derived from the newly launched SMOS (L-band) holds a better geographical coverage than X- and C-band products. Merlin et al. (2006) attempted to assimilate synthetic SMOS-type soil moisture observations into a distributed soil-vegetation-atmosphere transfer (SVAT) model. Land data assimilation with real SMOS soil moisture data has also started (e.g. De Lannoy et al., 2011; Zhan et al., 2012). The upcoming NASA Soil Moisture Active Passive (SMAP) mission is expected to further enhance the capability to estimate soil moisture, which will surely trigger more research efforts

**Table 5.** Summary of methods for snow representation in land/hydrologic models.

Models	Methods for simulating snow processes	References
A simple snowpack accumulation and melt model by Brasnett (1999)	Temperature index	Brasnett (1999)
A snowpack model developed by Clark et al. (2006)	Temperature index	Clark et al. (2006)
SNOW-17 model	Temperature index	Anderson (1973); Slater and Clark (2006)
SPH-AV snow model	Temperature index	Roy et al. (2010)
MIKE SHE model	Energy balance	Abbott et al. (1986)
A snow energy and mass balance model by Cline and Carroll (1999)	Energy balance	Cline and Carroll (1999)
Mosaic land surface model (LSM)	Energy balance	Rodell and Houser (2004)
Noah LSM	Energy balance	Ek et al. (2003); Zaitchik and Rodell (2009)
The Canadian Land Surface Scheme (CLASS)	Energy balance	Verseghy (2000)
The cold regions hydrological model (CRHM)	Energy balance	Pomeroy et al. (2007)
Catchment LSM	Energy balance (multiple layers)	Koster et al. (2000); Sun et al. (2004)
Community Land Model (CLM)	Energy balance (multiple layers)	Bonan et al. (2002); Su et al. (2008)
VIC model	Energy balance (multiple layers)	Andreadis and Lettenmaier (2006)

to assimilate new and potential satellite soil moisture into land/hydrologic models.

### 3 Snow cover and snow water equivalent

The presence of snow has a strong impact on the land surface energy and water budgets because of its high albedo, low thermal conductivity and water storage mechanism. In middle to high latitude or alpine river basins, spring and early summer runoff is usually dominated by snowmelt. Hence snow information is very important for numerical weather prediction and land/hydrologic models. In general, snow accumulation and ablation can be simulated either with an explicit description of heat and water exchange processes (an energy balance technique; e.g. Cline and Carroll, 1999; Verseghy, 2000) or using air temperature as the sole governing index (a temperature index method; e.g.

Brasnett, 1999; Slater and Clark, 2006) (Table 5).

Satellite remote sensing is capable of providing estimates on snow covered area (SCA) and snow water equivalent (SWE). The SCA can be estimated from snow reflectance characteristics in medium/high resolution visible and near-infrared observations (e.g. Moderate Resolution Imaging Spectroradiometer, MODIS; Advanced Very High Resolution Radiometer, AVHRR; Landsat Thematic Mapper, TM) (Hall et al., 2002; Painter et al., 2009; Rosenthal and Dozier, 1996; Zhao and Fernandes, 2009), while passive microwave sensors (e.g. AMSR-E, SMMR, SSM/I) can provide coarse-scale SWE estimation based upon a brightness temperature gradient between different microwave bands (e.g. Derksen, 2008; Derksen et al., 2003; Foster et al., 2005; Kelly, 2009; Kelly et al., 2003). A review of the typical sensors and retrieval algorithms for SCA

**Table 6a.** Summary of efforts to assimilate satellite snow cover into land/hydrologic models.

Authors	Satellite snow cover data	Data period	Land/hydrologic models	Assimilation methods	Study region
Rodell and Houser (2004)	MODIS daily snow cover 0.05° resolution product (MOD10C1)	1 January to 11 April 2003	Mosaic LSM	A rule-based direct insertion	Global/North America
Tang and Lettenmaier (2010)	MODIS daily snow cover 500 m resolution product (MOD10A1)	24 February 2000 to 31 December 2008	VIC model	A rule-based direct insertion	The Feather River Basin, California
Roy et al. (2010)	Daily SCA from MODIS (resolution: 500 m) and IMS (resolution: 4 km)	2004–2007 springs (25 March to 25 May)	The snow module SPH-AV in the hydrologic model MOHYSE	A direct insertion based on an empirical SWE threshold	The Du Nord watershed (1170 km <sup>2</sup> ) and the Aux Ecorces watershed (1110 km <sup>2</sup> ), Québec
Zaitchik and Rodell (2009)	MODIS daily snow cover 0.05° resolution product (MOD10C1)	September 2005 to June 2006 and September 2006 to June 2007	Noah LSM	Match the simulated snow with future satellite observations by adjusting the forcing air temperature and precipitation	Global
Andreadis and Lettenmaier (2006)	MODIS daily snow cover 500 m resolution product (MOD10A1)	4 consecutive winters (October 1999 to June 2003)	VIC model	EnKF	The US Snake River basin (280,000 km <sup>2</sup> )
Su et al. (2008, 2010)	MODIS daily 0.05° resolution SCF (MOD10C1)	January 2002 to June 2007	Community Land Model (CLM)	EnKF	North America
De Lannoy et al. (2012)	MODIS daily 500 m resolution SCF (MOD10A1-5)	2002–2010 winters (October–June)	Noah LSM	EnKF	A domain of ~75 × 100 km <sup>2</sup> in northern Colorado
Kolberg et al. (2006)	Landsat-7 ETM+ SCA (resolution: 30 m)	Two Landsat 7 ETM+ images acquired on 4 and 11 May 2000	A gridded distributed rainfall-runoff model	Update the snow depletion curve (SDC) state using a Bayesian scheme	The Vinstra and Sjoa catchments (60 × 40 km <sup>2</sup> ), central Norway

Abbreviations: VIC, the Variable Infiltration Capacity (VIC) model; SCA, Snow Covered Area; SCF, Snow Cover Fraction; SWE, Snow Water Equivalent; IMS, NOAA NESDIS Interactive Multisensor Snow and Ice Mapping System; EnKF, the Ensemble Kalman Filter.

**Table 6b.** Summary of efforts to assimilate satellite snow water equivalent (SWE) into land/hydrologic models.

Authors	Satellite SWE data	Data period	Land/hydrologic models	Assimilation methods	Study region
Andreadis and Lettenmaier (2006)	AMSR-E SWE retrievals (resolution: 25 km)	October 2003 to April 2004	VIC model	EnKF	The US Snake River basin (280,000 km <sup>2</sup> )
Dong et al. (2007)	SMMR-derived SWE (resolution: ~50 km)	1979–1987	Catchment LSM	EKF	North America
De Lannoy et al. (2010)	Synthetic AMSR-E SWE retrievals (resolution: 25 km)	30 September 2002 to 30 June 2003	Noah LSM	EnKF with different scaling schemes	A domain of ~75 × 100 km <sup>2</sup> in northern Colorado
De Lannoy et al. (2012)	AMSR-E Level-3 Daily Snow SWE product (resolution: 25 km)	2002–2010 winters (October–June)	Noah LSM	EnKF	A domain of ~75 × 100 km <sup>2</sup> in northern Colorado
Dechant and Moradkhani (2011)	AMSR-E brightness temperatures (36.5 GHz frequency at vertical polarization) (resolution: ~10 km)	1 December 2003 to 1 April 2004	The SNOW-17 model coupled with the SAC-SMA model	PF and EnKF	The East River watershed (754 km <sup>2</sup> ), Colorado

Abbreviations: AMSR-E, Advanced Microwave Scanning Radiometer for EOS; SMMR, Scanning Multichannel Microwave Radiometer; LSM, Land Surface Model; VIC, the Variable Infiltration Capacity (VIC) model; SAC-SMA, the Sacramento Soil Moisture Accounting Model; PF, the Particle Filter method; EnKF, the Ensemble Kalman Filter; EKF, the Extended Kalman Filter.

and SWE estimation was recently provided by Dietz et al. (2012).

During the past decade, much attention has been paid to the assimilation of satellite snow products into land/hydrologic models (Tables 6a and 6b). For example, snow cover estimated from visible and near-infrared satellite observations can be used to update the SWE simulations in land/hydrologic models through a rule-based direct insertion method. Rodell and Houser (2004) introduced MODIS-derived snow cover information into the Mosaic LSM based upon a direct insertion scheme. Specifically, given a location and time, if the LSM indicates snow but the MODIS snow cover value is very low (e.g. <10%), then the modeled SWE is adjusted to zero. Conversely, if the LSM does not show snow (i.e. SWE is 0) while MODIS provides a high snow cover (e.g. >40%), then a thin layer of snow is inserted into the model. A global simulation of the Mosaic LSM showed that such a simple updating approach could lead to improvement in the simulated SWE. Tang and Lettenmaier (2010) attempted to apply the 2000–2008 *Terra* MODIS daily snow cover 500 m resolution product (MOD10A1) to the Variable Infiltration Capacity (VIC) snow model with a similar updating technique. A case study of the Feather River Basin, California, indicated that the streamflow simulations during snow-melting intervals could be considerably affected by the addition of MODIS snow cover observations to the model. Roy et al. (2010) reported an improvement in spring streamflow simulations through a direct insertion of SCA products from MODIS and NOAA/NESDIS Interactive Multisensor Snow and Ice Mapping System (IMS), both separately and jointly, into the snow model component of a conceptual and lumped hydrologic model MOHYSE. In their scheme, the modeled SWE was adjusted to an empirical threshold value when the model and observation showed a contradiction. Although a direct insertion scheme

may be useful, a major deficit pertinent to its application is that the updating does not quantify the uncertainties in satellite observation and model. The adding or removing of the modeled snow guided by satellite observations with large random errors may produce non-physical snow estimation and therefore the dynamic imbalances in the model. To mitigate this problem, Zaitchik and Rodell (2009) proposed a so-called forward-looking assimilation scheme that sought an agreement between the modeled snow and future satellite observations by modifying the forcing air temperature and precipitation. The method was applied to assimilate MODIS SCA observations into the Noah LSM, which led to more accurate snow estimation than a direct-insert updating.

Andreadis and Lettenmaier (2006) used the EnKF method to assimilate MODIS-derived snow cover into the VIC macroscale hydrologic model. The satellite SCA observation was linked to the modeled SWE based upon a snow depletion curve (SDC). The assimilation of MODIS snow cover information improved the VIC SWE estimation, especially during snow-melt events. Su et al. (2008, 2010) also demonstrated that the assimilation of MODIS snow cover fraction (SCF) with the EnKF method could enhance the SWE simulations in the Community Land Model.

Landsat TM images have also proved effective in mapping snow covered fraction (e.g. Rosenthal and Dozier, 1996). Kolberg et al. (2006) assimilated the SCA data based on Landsat-7 Enhanced Thematic Mapper Plus (ETM+) imagery into the snow model component of a gridded distributed rainfall-runoff model. In the snow module, at each grid the snow state was represented by a snow depletion curve. A spatial model was proposed to provide the prior distribution of the snow depletion curves at all pixels, which was then updated based upon Bayes' theorem. A test over the central Norwegian high mountain region indicated

that the Bayesian assimilation of Landsat-7 ETM+ SCA significantly improved SWE estimation.

On the other hand, the SWE estimated by passive microwave sensors can be used to directly update the SWE simulations in land surface/hydrologic models (Table 6b). Andreadis and Lettenmaier (2006) attempted to assimilate AMSR-E SWE retrievals into the VIC model using the EnKF method, although the results did not show great promise. Generally, only a marginal enhancement in SWE simulations was found for shallow snowpacks after assimilating AMSR-E observations, while for deeper snowpacks the assimilation even produced larger SWE errors than the modeling without assimilation. In their defense, this was related to large biases in AMSR-E SWE retrievals. Dong et al. (2007) assimilated SMMR-derived SWE estimates into the Catchment LSM with the EKF. The SWE resulting from the assimilation, relative to those from the free-running model or SMMR alone, showed better agreement with in-situ observations. Similar to Andreadis and Lettenmaier (2006), Dong et al. (2007) also pointed out that the assimilation performance was not encouraging when remotely sensed SWE contained substantial errors or the simulated SWE values were very high. Dechant and Moradkhani (2011) assimilated AMSR-E brightness temperature data into a snow model (SNOW-17) to predict the spatial distribution of SWE. Their assimilation experiments indicated that the PF method led to more accurate SWE prediction than the EnKF. The snowmelt distribution derived from the assimilation could benefit streamflow forecasting in the SAC-SMA model.

More recently, progress has been made on the joint use of MODIS SCA and AMSR-E SWE products in hydrologic models. As examples, Kuchment et al. (2010) integrated the daily maps of both MODIS-derived SCA and AMSR-E-based SWE into a physically based snowpack model to obtain the spatial pattern of snowpack characteristics. The combination

of the two data sets proved useful for the snowmelt runoff hydrograph simulation in a physically based distributed hydrologic model. In the study of De Lannoy et al. (2012), multi-year data of AMSR-E SWE and MODIS SCF observations are assimilated separately and jointly into the Noah LSM with the EnKF technique. As shown for the shallow snowpack events, the joint AMSR-E SWE and MODIS SCF assimilation provided more realistic spatial SWE patterns than when the two data sets were assimilated separately.

In addition to land data assimilation usage, remote sensing snow products have also been used for model initialization and calibration. For example, Tekeli et al. (2005) used the snow depletion curves derived from the MODIS 8-day snow cover product (MOD10A2) to initialize a snowmelt runoff model, and demonstrated that MODIS could provide reliable SCA estimation for the simulations and prediction of snowmelt runoff. Parajka and Blöschl (2008) showed that MODIS snow cover products could be used for the calibration of a semi-distributed hydrologic model, which resulted in an improved runoff modeling.

#### *4 Leaf area index*

Leaf area index (LAI) plays a critical role in estimating the amount of precipitation interception and evapotranspiration (ET). LAI can be estimated from visible/near-infrared satellite observations (e.g. Chen and Cihlar, 1996; Tucker et al., 2005) or using active LiDAR or radar systems (e.g. Manninen et al., 2005; Morsdorf et al., 2006). The LAI data, which were derived from NOAA-AVHRR NDVI (normalized difference vegetation index) observations, were utilized as inputs to a large-scale hydrologic modeling in the Senegal River Basin with MIKE SHE (Andersen et al., 2002; Stisen et al., 2008). The application of AVHRR LAI observations in MIKE SHE exerted a substantial impact on the hydrograph and

evapotranspiration simulations. The prediction of discharge was considerably improved, and the relative contribution of each component to the total evapotranspiration was remarkably changed. Droogers and Kite (2002) explored the potential of improving hydrologic modelling at different spatial scales (field, irrigation scheme, and basin) using AVHRR LAI data. The study suggested that the use of AVHRR LAI measurements, in combination with other public domain data, in the SWAP (soil–water–atmosphere–plant) and SLURP (semi-distributed, land-use-based, runoff processes) models could provide a powerful tool for water resources assessment.

A distributed hydrology-vegetation model utilized the vegetation characteristics and LAI estimated from Landsat TM as inputs to predict evapotranspiration (Chen et al., 2005). An experiment based on a small watershed in Saskatchewan, Canada, indicated that the mapped ET results were similar to eddy-covariance ET measurements recorded within the watershed. As shown in Boegh et al. (2004), the LAI data based upon Landsat TM and SPOT measurements were employed to adjust the LAI simulated by a coupled Daisy/MIKE SHE model. The remote sensing-based average LAI was estimated for each agro-hydrologic group response unit. The simulated LAI was then adjusted based upon the remotely sensed LAI. As a result, the prediction of evapotranspiration and crop yields was improved, although the ET simulation suffered from the large-scale spatial variation in LAI.

The MODIS sensor aboard NASA's *Terra* and *Aqua* satellites offers an efficient remote sensing tool for deriving LAI (e.g. Fensholt et al., 2004; Huete et al., 2002; Myneni et al., 2002). Over the last decade, MODIS-based LAI measurements have been frequently utilized as one of the input data sources for driving distributed hydrologic models (Table 7). In particular, a combination of MODIS-based LAI and hydrologic models has the potential of improving ET estimation. Zhang

and Wegehenkel (2006) incorporated MODIS LAI data into a grid-based soil water balance model to estimate the spatial patterns of daily soil moisture and actual evapotranspiration. The 8-day LAI (MOD15A2) and 16-day NDVI (MOD13A2) products at a spatial resolution of 1000 m were used to initialize the modeling. Overall, the simulated soil water content and actual ET rates were shown to be in good agreement with in-situ observations. Andersen (2008) demonstrated that MODIS-derived LAI data (MOD15A2) were well suited for use in the SVAT (Soil Vegetation Atmosphere Transfer) model (coupled with MIKE SHE) to simulate ET. Boegh et al. (2009) presented the use of MODIS NDVI and LAI products in a physically based agro/ecohydrologic model (Daisy) for evapotranspiration and runoff simulations at a wide range of spatial scales (agricultural, forest, and urban land surfaces). The study concluded that much of the observed variability of streamflow and eddy covariance latent heat fluxes could be captured by the Daisy modeling system when both the model and remote sensing data are available at appropriate scale to resolve spatial variations in land surface features.

The assimilation of remote sensing-derived LAI in hydrologic models has also emerged over the last decade. A constant gain Kalman filter method was adopted by Vazifedoust et al. (2009) to assimilate MODIS-based LAI in a distributed SWAP model. The LAI data were derived from 250 m spatial resolution MODIS observations of the soil-adjusted vegetation index based upon a logarithmic relation between the two types of data sets. The study showed that the assimilation of MODIS-based LAI could result in better ET and crop yield forecasts in the SWAP model.

## 5 Evapotranspiration

Evapotranspiration, accounting for precipitation interception, land surface evaporation, and plant transpiration, is an essential part of the

**Table 7.** Representative efforts to integrate MODIS-based leaf area index (LAI) and land/hydrologic models.

Authors	LAI data	Data period	Land/hydrologic models	Integration methods	Study region
Zhou et al. (2004)	MOD15A2 (MODIS 8-day LAI) product (resolution: 1 km)	Over 2000	The three-layer variable infiltration capacity (VIC-3L) model	MODIS LAI used as model inputs	The Baohe River basin (drainage area of ~2500 km <sup>2</sup> ), China
Zhang and Wegehenkel (2006)	MODIS 16-day NDVI (MOD13A2) and 8-day LAI (MOD15A2) (resolution: 1 km)	1 January 2001 to 31 December 2003	A grid-based soil water balance model	Model inputs	The Ucker catchment (2415 km <sup>2</sup> ) in northeastern Germany
Andersen (2008)	MOD15A2 product (resolution: 1 km)	1 October 2005 to 30 September 2006	MIKE SHE SVAT (Soil Vegetation Atmosphere Transfer) model	Model inputs	The Andarax River basin (2265 km <sup>2</sup> ), Spain
Boegh et al. (2009)	LAI based upon MODIS 500 m (MOD13A1) and 1 km (MOD13A2) NDVI	2001–2002 growing seasons	The agro-hydrological model Daisy	The LAI simulation was adjusted to match MODIS LAI	The island of Sjælland (7330 km <sup>2</sup> ), Denmark
Vazifedoust et al. (2009)	LAI based upon 250 m MODIS estimation of SAVI (soil-adjusted vegetation index)	March to May 2005	The physically based soil–water–atmosphere–plant (SWAP) model	Assimilation with a Kalman filter	The Borkhar irrigation district (833 km <sup>2</sup> ), Iran
T. Liu et al. (2012)	LAI based upon MODIS NDVI (resolution: 1 km)	1 May to 31 December 2005	MIKE SHE	Model inputs	The Tarim River basin in China (the model domain is 132,800 km <sup>2</sup> )

hydrologic cycle. Evapotranspiration rates are subject to meteorological factors, soil characteristics, vegetation, surface parameters, etc., and therefore usually exhibit substantial spatial variability. Remote sensing cannot provide a direct measurement of evapotranspiration. Surface energy balance models are usually required to estimate ET from satellite measurements. Satellite thermal infrared and optical data are suitable for estimating evapotranspiration (e.g. Bastiaanssen et al., 1998; Jiang and Islam, 2001; Loheide and Gorelick, 2005; Stisen et al., 2008). Potential evapotranspiration (PET) can be derived from satellite estimation of surface radiation (Makkink, 1957). Radiation-based PET derived from geostationary satellite visible/infrared data has been used as one of key inputs to large-scale hydrologic modeling over the last decade (e.g. Shu et al., 2010; Stisen et al., 2008). Satellite observations of NDVI and LAI can also be used to estimate PET. Zhou et al. (2006) demonstrated the potential of AVHRR NDVI data to provide PET for a distributed hydrologic model.

Boegh et al. (2004) utilized evapotranspiration rates, which are calculated based upon surface and radiation parameters derived from Landsat TM and SPOT data, to validate ET simulated by a coupled Daisy-MIKE SHE model. The result showed good agreement between the simulated ET and remote sensing measurements. Kamble and Irmak (2008) attempted to assimilate ET, which was derived from Landsat TM/ETM data with a surface energy balance model, into a SWAP model. The assimilation of Landsat-based ET using genetic algorithms led to a moderate enhancement in the SWAP's capability to predict soil moisture.

MODIS data in combination with the Surface Energy Balance Algorithm for Land (SEBAL; e.g. Bastiaanssen et al., 1998) are able to provide actual ET for hydrologic modeling (Table 8). SEBAL solves the energy budget equation by converting satellite radiances into land surface

heat and vegetation parameters. Immerzeel and Droogers (2008) demonstrated the capability of MODIS/SEBAL-derived ET to calibrate the SWAT (Soil and Water Assessment Tool) model that can simulate, on a daily time step, the hydrologic processes involving rainfall, surface runoff, subsurface flow, groundwater, and evapotranspiration (Arnold and Fohrer, 2005). To minimize the difference between the measured and modeled ET values, a non-linear parameter estimation algorithm was built to adjust some model parameters and inputs such as land use, soil, or precipitation via a number of optimization runs based upon different parameter combinations. As shown for the best optimization run, the correlation between the simulated and observed actual ET was significantly improved.

Qin et al. (2008) attempted to predict the water balance for the Haihe River basin by assimilating MODIS-based ET by the SEBS (Surface Energy Balance System algorithm; Su, 2002) into a physically based distributed model. The assimilation using the EKF technique was shown to be superior to the open loop (free-run) in mapping the finescale structure of actual ET. Vazifedoust et al. (2009) assimilated MODIS/SEBAL-derived relative evapotranspiration (the ratio of actual ET and PET) into the SWAP model using a constant gain Kalman filter method. Results showed that the assimilation of MODIS-based relative ET information produced only a marginal impact upon the simulated LAI and crop yield.

In addition to SEBAL, other algorithms have also been developed to estimate actual ET from MODIS observations, e.g. the Penman-Monteith equation (Leuning et al., 2008). Zhang et al. (2009) explored the use of remote sensing-based actual ET, which was derived from MODIS LAI data using the Penman-Monteith equation, in a lumped-type rainfall-runoff modeling. More accurate runoff simulations in ungauged catchments were produced on a daily and a monthly basis when the model was calibrated with both MODIS-based actual ET and the observed

**Table 8.** Representative studies of integrating MODIS-based evapotranspiration (ET) and land/hydrologic modeling.

Authors	ET data	Data period	Land/hydrologic models	Integration methods	Study region
Immerzeel and Droogers (2008)	MODIS/SEBAL-derived actual ET (resolution: 1 km)	October 2004 to May 2005	The SWAT (Soil and Water Assessment Tool) model	Model calibration	The Upper Bhima catchment (45,678 km <sup>2</sup> ) in southern India
Qin et al. (2008)	MODIS-based ET using the SEBS algorithm by Su (2002) (resolution: 1 km)	Year 2005	A distributed model WEP-L (Water and Energy transfer Process in Large river basins)	Assimilation with an extended Kalman filter	The Haihe River basin (317,800 km <sup>2</sup> ), China
Vazifedoust et al. (2009)	MODIS/SEBAL-derived relative ET (the ratio of actual and potential ET) (resolution: 1 km)	15 dates during the 2005 winter growing season	The physically based soil-water-atmosphere-plant (SWAP) model	Assimilation with a Kalman filter	The Borkhar irrigation district (833 km <sup>2</sup> ), Iran
Zhang et al. (2009)	ET based upon MODIS LAI (MOD15A2) using the Penman-Monteith equation (resolution: 1 km)	2001 to 2005	A lumped daily rainfall-runoff model SIMHYD	Model calibration	120 catchments (ranging from 50 to 2000 km <sup>2</sup> ) in southeast Australia
T. Liu et al. (2012)	MODIS-based actual ET using the algorithm by Verstraeten et al. (2005) (resolution: 5 km)	1 May to 31 December 2005	MIKE SHE	Model inputs	The Tarim River basin in China (the model domain is 132,800 km <sup>2</sup> )

streamflow as compared to the calibration using only the streamflow measurements.

## IV Discussion

This paper provides the status of integrating land/hydrologic models and remotely sensed hydrologic products (precipitation, surface soil moisture, SCA, SWE, LAI, and ET) over the past decade. The main efforts in this field include: (1) the use of satellite and radar precipitation data in driving hydrologic models; (2) the assimilation of microwave soil moisture products (mainly from SMMR, AMSR-E, and ASCAT) in land surface and hydrologic models to update soil moisture simulations or to identify antecedent soil moisture conditions; (3) the assimilation of MODIS snow cover and AMSR-E SWE in land models; and (4) the model calibration, initialization, and validation using LAI and ET derived from optical observations (mainly MODIS, AVHRR, and Landsat TM) and their preliminary assimilation. These studies have suggested that the integration of remote sensing data and land/hydrologic modeling can offer benefits to hydrologic forecasts, especially through advanced data assimilation methods. In practice, however, the integration of remote sensing and land/hydrologic modeling is often complex, and has faced a number of critical problems and challenges.

### *I Considerable uncertainties and biases in remotely sensed products*

Since the hydrology and Earth system contains various complex, non-linear stochastic processes, subtle errors in the forcing fields can cause very large uncertainties in model outputs. Hence, the quality (both accuracy and precision) of remote sensing-based hydrologic variables exerts a critical impact on the predictive capability of hydrologic and land surface models. Remotely sensed products usually contain substantial uncertainties and biases, which

depend on a wide range of factors, such as sensor type (wavelength, resolution, polarization, etc.), cloud cover, vegetation cover, retrieval algorithm, and physical connection between retrievals and measurements. To improve retrievals from remote sensing measurements, an efficient way is to use multi-sensors (including in-situ measurements-adjusted remotely sensed products). For example, satellite precipitation can be estimated from visible/infrared and microwave measurements. However, each sensor type may suffer from its weakness inherent in measurements (Table 2). Microwave sensors onboard polar-orbiting satellites can directly detect precipitation hydrometeors and the overlying cloud layer, but generally have relatively coarse spatial (10–20 km) and temporal (1–2 visits per day) sampling frequency. The visible/infrared measurements from geostationary satellites can offer a much higher time resolution (hourly or finer), but have a poor physical connection to precipitation since rainfall rates are derived from cloud-top temperatures. A combination of the visible/infrared and passive microwave techniques could counteract the shortcomings in each product/sensor type and produce a more reliable high spatial and temporal resolution precipitation field (e.g. Huffman et al., 2007; Joyce et al., 2004), which may be more appropriate for driving high-resolution distributed hydrologic models (e.g. Pereira-Cardenal et al., 2011). Kitzmiller et al. (2011) demonstrated that QPE from the merged satellite-radar-gauge observations had the better potential to improve finescale hydrologic modeling.

New sensor technologies can improve the accuracy of remote sensing retrievals. For example, as indicated by some studies (e.g. Ryzhkov et al., 2005), polarimetric radars can effectively identify the variability of raindrop size distribution and therefore improve rainfall estimation. For surface soil moisture estimation, the recently launched L-band sensor SMOS/MIRAS (Kerr et al., 2012) is more effective in vegetated regions than those operating at higher

microwave frequencies (e.g. X- and C-band AMSR-E observations).

Advanced data assimilation schemes can optimally merge remote sensing observations into models by taking into account the model and measurement uncertainties. For instance, Francois et al. (2003) showed that a direct insertion of ERS-1 SAR-derived soil moisture into a lumped rainfall-runoff model did not improve streamflow prediction. By contrast, the sequential assimilation of SAR soil moisture with the EKF method had the potential to constrain the uncertainties in the forcing data and the model, thus improving runoff simulations. Note that advanced data assimilation schemes measure only random observational errors, and biases (systematic errors) in remotely sensed products will impact their ability to produce the best estimate. For example, large biases contained in the AMSR-E SWE product did not cause satisfactory assimilation outcomes (Andreadis and Lettenmaier, 2006). If observations biases are known, they should be removed prior to the assimilation. Unfortunately biases in remotely sensed products are difficult to estimate in practice due to their complicated variations in space and time. The development of bias correction schemes is an important ongoing research activity.

## 2 The model-measurement scale discrepancy

Surface soil moisture and SWE derived from spaceborne passive microwave sensor observations (e.g. AMSR-E, SMMR, SSM/I, SMOS) are of particular value for land/hydrologic modeling, but typically have a relatively coarse spatial resolution (>25 km). With the rapid increase in computing power, on the other hand, the operational distributed hydrologic/land surface models can be available at very high resolution ( $\leq 1$  km in space). This results in an increased demand for integrating coarse-scale remote sensing products and finescale land/hydrologic simulations. Traditionally, coarse resolution observations are

disaggregated into the finer model grids prior to being added into the model (e.g. Andreadis and Lettenmaier, 2006; Merlin et al., 2006). This simplistic treatment may be useful, but the interpolation errors contained in the disaggregated products are likely to be introduced to the model.

A combination of remotely sensed products across different spatial scales can be used to improve an *a priori* disaggregation scheme that resamples coarse-scale observations into the finescale model grids prior to data assimilation. As we know, for example, satellite snow products typically include snow cover from visible/near-infrared observations (e.g. MODIS, AVHRR, Landsat TM) and SWE from passive microwave sensors (e.g. AMSR-E, SMMR, SSM/I). Snow cover data usually have a good spatial resolution (<1 km), but are valid only for daytime and cloud-free conditions, while microwave SWE estimates hold the advantage of continuous coverage during day/night, but generally suffer from their relatively coarse spatial resolution. Merging coarse-scale microwave SWE measurements with finescale visible/near-infrared snow cover data (e.g. Gao et al., 2010; Liang et al., 2008) could produce more reliable disaggregated snow products for high resolution distributed hydrologic simulations (e.g. Kongoli et al., 2007).

Modern data assimilation provides an effective framework for directly merging satellite measurements and models that differ in resolution/scale. De Lannoy et al. (2010) investigated the assimilation of synthetic coarse-scale microwave SWE observations into the finescale Noah LSM with the EnKF. The study assessed two downscaling schemes: a direct assimilation of coarse-scale observations by the use of a scaling observation operator and a disaggregation of coarse-scale observations to the finescale model grids prior to data assimilation. Results showed that the direct assimilation approach was more efficient than the prior disaggregation scheme. The use of an influence radius (i.e. inclusion of observations from neighboring pixels) could improve the assimilation performance in both schemes. A joint

assimilation of multi-sensor observations proved to be the most efficient in simulating both the overall and finescale structures of land variables (e.g. De Lannoy et al., 2012; Draper et al., 2012).

### **3 Statistical biases between remotely sensed and modeled state variables**

Theoretically, advanced assimilation schemes can dynamically integrate remote sensing observations and model simulations to produce an optimal estimate of the state variable of interest. In reality, however, the assimilation of remote sensing data in land/hydrologic models may be complex because of inherent differences between remote sensing and model simulations. Remote sensing is an indirect measurement of land and hydrologic parameters, and reflects only instantaneous 'true' values of the object within the sampled area (instantaneous field of view, IFOV) at the observing time. By contrast, a model simulates the state of hydrologic and land parameters at desired spatial and temporal scales based upon their continuous evolution in time and space, which is governed by internal physics processes and dynamic mechanisms, initial conditions, and forcing (boundary conditions). Hence statistical differences between remotely sensed and modeled variables are very likely.

For instance, satellite-based and modeled soil moisture showed different mean value and probability distribution (Reichle and Koster, 2004; Reichle et al., 2004), which could be a major impediment for optimally merging the two data sets. To mitigate the satellite-model biases impact on satellite soil moisture assimilation, a priori observation rescaling by matching the cumulative distribution functions of the two data sets could be useful and practical (Crow et al., 2009; Draper et al., 2012; Reichle and Koster, 2004, 2005), although new random errors generated in satellite products due to rescaling cannot be entirely ruled out. Another method to remove the biases is

that the land/hydrologic model is calibrated using the climatology of satellite soil moisture observations, but the optimized model parameters may show large spatial variability than those based upon the traditional soil texture (Kumar et al., 2012).

### **4 Difficulty in quantifying observation error covariances**

In a data assimilation system, the input error covariances reflect the uncertainties (random errors) in model forecast (background) and observation, and strongly affect to what extent the forecast will be modified to fit the observations. Their accurate specification is therefore crucial to the success of the analysis. Observation error covariances usually result from both instrumental errors and representativeness errors. The former can be estimated according to the precision of a measurement instrument, while the latter are caused mainly by the misfit between an observation space and a model space. Since remote sensing observations are indirect measurements, their preprocessing (retrieval and interpolation algorithms) will introduce substantial representativeness errors and error correlations. Further, if the retrieval procedure involves the background information, the observation and the background errors will be not completely independent. Hence the estimate of representativeness errors is critically important to the assimilation of remote sensing data. In reality, however, these error characteristics are complex, and are difficult or impossible to completely estimate since they are subject to a number of factors (platform, vegetation cover, observation operator, regridding, etc.). Some approximations could be efficient. For example, the error probability densities are assumed to be Gaussian, and observation error correlations are assumed to be zero, although such approximations will raise other problems (discussed below).

### 5 Limitation of Gaussian assumption

Data assimilation provides a framework for optimally merging remotely sensed observations and land/hydrologic modeling, and represents the current state-of-the art in quantitative use of remotely sensed data in models. The Earth and hydrologic system is dominated by various non-linear stochastic processes, which in turn are affected by noise sources. In this way, a general land/hydrologic data assimilation problem can be described as estimating the probability density function (PDF) of the underlying system based upon the model prediction and the observation. The solutions to the problem can be represented by statistical parameters, such as means, medians, modes, or variances. Bayesian filtering is optimal for seeking the posterior PDF conditioned on the observations (Gordon et al., 1993; Malakoff, 1999). When it comes to assimilating remotely sensed hydrologic products into land surface/hydrologic models, the KF and its variants (EKF, EnKF) have been dominantly employed in this field over the past decade. The KF can be viewed as a special case of Bayesian filtering under the linear/Gaussian (i.e. normal distribution) situation. In other words, the KF is based upon the assumption of linear systems and Gaussian distributions in the predicted and measured error statistics. Its variants (e.g. EKF, EnKF) can solve the optimal estimation problem for some non-linear systems, but still hold the Gaussian assumption. In reality, however, non-linear, non-Gaussian circumstances are the most common. In a non-linear system, the non-Gaussian forecast errors could be produced as the system evolves even if the error distributions are initially Gaussian (Evensen and van Leeuwen, 2000; Miller et al., 1999). The EKF often fails to track the state space in a strongly non-linear system which has a highly skewed PDF (e.g. Miller et al., 1999).

The EnKF usually performs better than the EKF for high dimension systems since the

former uses a Monte Carlo method, instead of a linearized and approximate error covariance equation in the latter, to solve the Fokker-Planck equation for the time evolution of the model state PDF. Nevertheless, the EnKF scheme may also fail in cases where a satisfactory estimator cannot always be well represented by the ensemble mean (e.g. Bengtsson et al., 2003). Reichle et al. (2002) showed that due to the impact of model non-linearity, the PDF of the modeled soil moisture under very wet or dry states became skewed, and was far from Gaussian. In this situation, the EnKF could not provide an optimal estimation since the analysis step ignored the asymmetric distribution and used only the first two moments (the mean and the covariance) of the PDF. Crow and Wood (2003), in their brightness temperature assimilation experiments for soil moisture estimation, also suggested that the EnKF may not yield satisfactory results when the underlying error structures are significantly non-Gaussian.

A general non-linear filter (non-linear/non-Gaussian) is expected to be efficient when used for the non-linear dynamic models with considerably skewed PDF for the predicted errors (e.g. multi-modal structure) (Han and Li, 2008; Miller et al., 1999). Non-linear/non-Gaussian filters can be implemented through particle interpretations (e.g. Pham, 2001) or kernel approximation (Miller et al., 1999). For example, the PF method uses a set of particles (sampled from a proposal distribution) with associated importance weights to approximate the posterior PDF. In theory, the PF is suitable for all types of systems (linear or non-linear) and PDFs (Gaussian or non-Gaussian) due to the ability to track the full state space (Arulampalam et al., 2002). Some researchers have conducted satellite snow assimilation with the PF (e.g. Dechant and Moradkhani, 2011) and the preliminary results showed promise.

## V Conclusions

Studies have suggested that remote sensing data hold great potential to improve the predictive capability of land/hydrologic models, especially through advanced data assimilation schemes. The encouraging results will warrant further research efforts in integrating remotely sensed products and land/hydrologic models. Future research directions should be focused upon the following: (1) development of techniques to combine multiple and complementary remote sensing sources to provide the disaggregated products for hydrologic modeling; (2) joint assimilation of multi-scale, multi-sensor products in land/hydrologic models; (3) application of general data assimilation approaches (e.g. non-linear/non-Gaussian filters); (4) further development of the techniques that are suitable for satellite LAI and ET data assimilation; (5) integration of new and potential sensor products (e.g. soil moisture from the planned SMAP mission; snow water equivalent from AMSR2) with land/hydrologic models.

## Acknowledgements

Sincere thanks to the two anonymous reviewers for their helpful comments on the original manuscript. The lead author is generously supported through an NSERC CGSD and a Meteorological Service of Canada Graduate Supplement.

## Funding

The author(s) received no financial support for the research, authorship, and/or publication of this article.

## References

- Abbott MB, Bathurst JC, Cunge JA, et al. (1986) An introduction to the European hydrological system – système hydrologique Européen, ‘SHE’, 2: Structure of a physically-based, distributed modeling system. *Journal of Hydrology* 87: 61–77.
- Albergel C, Rudiger C, Carrer D, et al. (2009) An evaluation of ASCAT surface soil moisture products with in-situ observations in southwestern France. *Hydrology and Earth System Sciences* 13: 115–124.
- Andersen FH (2008) Hydrological modeling in a semi-arid area using remote sensing data. PhD thesis, University of Copenhagen.
- Andersen J, Dybkjaer G, Jensen KH, et al. (2002) Use of remotely sensed precipitation and leaf area index in a distributed hydrological model. *Journal of Hydrology* 264: 34–50.
- Anderson EA (1973) National weather service river forecast system – snow accumulation and ablation model. Technical Memo NWS HYDRO-17. Silver Spring, MD: National Oceanic and Atmospheric Administration (NOAA), 217 pp.
- Andreadis KM and Lettenmaier DP (2006) Assimilating remotely sensed snow observations into a macroscale hydrology model. *Advances in Water Resources* 29: 872–886.
- Arnold JG and Fohrer N (2005) SWAT2000: Current capabilities and research opportunities in applied watershed modeling. *Hydrological Processes* 19: 563–572.
- Arulampalam MS, Maskell S, Gordon N, et al. (2002) A tutorial on particle filters for online nonlinear/non-Gaussian Bayesian tracking. *IEEE Transactions on Signal Processing* 50: 174–188.
- Bartalis Z, Wagner W, Naeimi V, et al. (2007) Initial soil moisture retrievals from the METOP-A Advanced Scatterometer (ASCAT). *Geophysical Research Letters* 34: L20401.
- Bastiaanssen WGM, Menenti M, Feddes RA, et al. (1998) A remote sensing surface energy balance algorithm for land (SEBAL). 1. Formulation. *Journal of Hydrology* 213: 198–212.
- Bates BC, Kundzewicz ZW, Wu S, et al. (eds) (2008) Climate change and water. Technical Paper of the Intergovernmental Panel on Climate Change. Geneva: IPCC Secretariat.
- Bengtsson T, Snyder C and Nychka D (2003) Toward a nonlinear ensemble filter for high-dimensional systems. *Journal of Geophysical Research* 108(D24): 8775–8785.
- Biggs EM and Atkinson PM (2011) A comparison of gauge and radar precipitation data for simulating an extreme hydrological event in the Severn Uplands, UK. *Hydrological Processes* 25: 795–810.
- Bindlish R, Crow WT and Jackson TJ (2009) Role of passive microwave remote sensing in improving flood forecasts. *IEEE Geoscience and Remote Sensing Letters* 6: 112–116.

- Bindlish R, Jackson TJ, Wood E, et al. (2003) Soil moisture estimates from TRMM microwave imager observations over the Southern United States. *Remote Sensing of Environment* 85: 507–515.
- Boegh E, Poulsen RN, Butts M, et al. (2009) Remote sensing based evapotranspiration and runoff modeling of agricultural, forest and urban flux sites in Denmark: From field to macro-scale. *Journal of Hydrology* 377: 300–316.
- Boegh E, Thorsen M, Butts MB, et al. (2004) Incorporating remote sensing data in physically based distributed agro-hydrological modeling. *Journal of Hydrology* 287: 279–299.
- Bonan K, Oleson W, Vertenstein M, et al. (2002) The land surface climatology of the community land model coupled to the NCAR community climate model. *Journal of Climate* 15: 3123–3149.
- Borga M (2002) Accuracy of radar rainfall estimates for streamflow simulation. *Journal of Hydrology* 267: 26–39.
- Brasnett B (1999) A global analysis of snow depth for numerical weather prediction. *Journal of Applied Meteorology* 38: 726–740.
- Brocca L, Melone F, Moramarco T, et al. (2010) Improving runoff prediction through the assimilation of the ASCAT soil moisture product. *Hydrology and Earth System Sciences* 14: 1881–1893.
- Butts MB, Overgaard J, Viaene P, et al. (2005) Flexible process-based hydrological modeling framework for flood forecasting-MIKE SHE. Paper presented at the International Conference ‘Innovation, advances and implementation of flood forecasting technology’, 17–19 October, Tromsø, Norway.
- Chen JM and Cihlar J (1996) Retrieving leaf area index of boreal conifer forests using Landsat TM images. *Remote Sensing of Environment* 55: 153–162.
- Chen JM, Chen XY, Ju WM, et al. (2005) Distributed hydrological model for mapping evapotranspiration using remote sensing inputs. *Journal of Hydrology* 305: 15–39.
- Clark MP, Slater AG, Barrett AP, et al. (2006) Assimilation of snow covered area information into hydrologic and land-surface models. *Advances in Water Resources* 29: 1209–1221.
- Cline DW and Carroll TR (1999) Inference of snow cover beneath obscuring clouds using optical remote sensing and a distributed snow energy and mass balance model. *Journal of Geophysical Research* 104(D16): 19631–19644.
- Cole SJ and Moore RJ (2008) Hydrological modeling using raingauge- and radar-based estimators of areal rainfall. *Journal of Hydrology* 358: 159–181.
- Cole SJ and Moore RJ (2009) Distributed hydrological modeling using weather radar in gauged and ungauged basins. *Advances in Water Resources* 32: 1107–1120.
- Collier CG (2009) On the propagation of uncertainty in weather radar estimates of rainfall through hydrological models. *Meteorological Applications* 16: 35–40.
- Crosson WL, Laymon CA, Inguva R, et al. (2002) Assimilating remote sensing data in a surface flux-soil moisture model. *Hydrological Processes* 16: 1645–1662.
- Crow WT and Ryu D (2009) A new data assimilation approach for improving runoff prediction using remotely-sensed soil moisture retrievals. *Hydrology and Earth System Sciences* 13: 1–16.
- Crow WT and Wood EF (2003) The assimilation of remotely sensed soil brightness temperature imagery into a land surface model using Ensemble Kalman filtering: A case study based on ESTAR measurements during SGP97. *Advances in Water Resources* 26: 137–149.
- Crow W and Zhan X (2007) Continental-scale evaluation of remotely sensed soil moisture products. *IEEE Geoscience and Remote Sensing Letters* 4: 451–455.
- Crow WT, Bindlish R and Jackson TJ (2005) The added value of spaceborne passive microwave soil moisture retrievals for forecasting rainfall-runoff ratio partitioning. *Geophysical Research Letters* 32: L18401.
- Crow WT, Huffman GH, Bindlish R, et al. (2009) Improving satellite-based rainfall accumulation estimates using spaceborne surface soil moisture retrievals. *Journal of Hydrometeorology* 10: 199–212.
- Dechant C and Moradkhani H (2011) Radiance data assimilation for operational snow and streamflow forecasting. *Advances in Water Resources* 34: 351–364.
- De Lannoy GJM, Reichle RH, Arsenault KR, et al. (2012) Multiscale assimilation of Advanced Microwave Scanning Radiometer-EOS snow water equivalent and Moderate Resolution Imaging Spectroradiometer snow cover fraction observations in northern Colorado. *Water Resources Research* 48: W01522.
- De Lannoy GJM, Reichle RH, Draper C, et al. (2011) Assimilation of SMOS surface soil moisture retrievals into the Catchment land surface model. Invited presentation at the AGU Fall Meeting, San Francisco.
- De Lannoy GJM, Reichle RH, Houser PR, et al. (2010) Satellite-scale snow water equivalent assimilation into

- a high-resolution land surface model. *Journal of Hydrometeorology* 11: 352–369.
- Derksen C (2008) The contribution of AMSR-E 18.7 and 10.7 GHz measurements to improved boreal forest snow water equivalent retrievals. *Remote Sensing of Environment* 112: 2701–2710.
- Derksen C, Walker A, Ledrew E, et al. (2003) Combining SMMR and SSM/I data for time series analysis of central North American snow water equivalent. *Journal of Hydrometeorology* 4: 304–316.
- Dietz AJ, Kuenzer C, Gessner U, et al. (2012) Remote sensing of snow – a review of available methods. *International Journal of Remote Sensing* 33(13): 4094–4134.
- Dong J, Walker JP, Houser PR, et al. (2007) Scanning multichannel microwave radiometer snow water equivalent assimilation. *Journal of Geophysical Research* 112: D07108.
- Dorigo WA, Zurita-Milla R, de Wit AJW, et al. (2007) A review on reflective remote sensing and data assimilation techniques for enhanced agroecosystem modeling. *International Journal of Applied Earth Observation and Geoinformation* 9: 165–193.
- Draper CS, Mahfouf J-F and Walker JP (2009) An EKF assimilation of AMSR-E soil moisture into the ISBA land surface scheme. *Journal of Geophysical Research* 114: D20104.
- Draper CS, Reichle RH, De Lannoy GJM, et al. (2012) Assimilation of passive and active microwave soil moisture retrievals. *Geophysical Research Letters* 39: L04401.
- Droogers P and Kite G (2002) Remotely sensed data used for modeling at different hydrological scales. *Hydrological Processes* 16: 1543–1556.
- Ek M, Mitchell K, Yin L, et al. (2003) Implementation of Noah land surface model advances in the National Centers for Environmental Prediction operational mesoscale Eta model. *Journal of Geophysical Research* 108: 8851.
- Evensen G and van Leeuwen PJ (2000) An Ensemble Kalman Smoother for nonlinear dynamics. *Monthly Weather Review* 128: 1852–1867.
- Fensholt R, Sandholt I and Rasmussen MS (2004) Evaluation of MODIS LAI, fAPAR and the relation between fAPAR and NDVI in a semi-arid environment using in situ measurements. *Remote Sensing of Environment* 91: 490–507.
- Foster JL, Sun C, Walker JP, et al. (2005) Quantifying the uncertainty in passive microwave snow water equivalent observations. *Remote Sensing of Environment* 94: 187–203.
- Francois C, Quesney A and Otle C (2003) Sequential assimilation of ERS-1 SAR data into a coupled land surface–hydrological model using an extended Kalman filter. *Journal of Hydrometeorology* 4: 473–487.
- Gao Y, Xie H, Yao T, et al. (2010) Integrated assessment on multi-temporal and multi-sensor combinations for reducing cloud obscuration of MODIS snow cover products of the Pacific Northwest USA. *Remote Sensing of Environment* 114: 1662–1675.
- Germann U, Berenguer M, Sempere-Torres D, et al. (2009) REAL-Ensemble radar precipitation estimation for hydrology in a mountainous region. *Quarterly Journal of the Royal Meteorological Society* 135: 445–456.
- Gillijns S and De Moor B (2007) Model error estimation in ensemble data assimilation. *Nonlinear Processes in Geophysics* 14: 59–71.
- Gordon NJ, Salmond DJ and Smith AFM (1993) Novel approach to nonlinear/non-Gaussian Bayesian state estimation. *IEEE Proceedings on Radar and Signal Processing* 140: 107–113.
- Grimes DIF and Diop M (2003) Satellite-based rainfall estimation for river flow forecasting in Africa. I: Rainfall estimates and hydrological forecasts. *Hydrological Sciences Journal (Journal des Sciences Hydrologiques)* 48: 567–584.
- Guo J, Liang X and Leung LR (2004) Impacts of different precipitation data sources on water budgets. *Journal of Hydrology* 298: 311–334.
- Habib E, Aduvala AV and Meselhe EA (2008a) Analysis of radar-rainfall error characteristics and implications for streamflow simulation uncertainty. *Hydrological Sciences Journal (Journal des Sciences Hydrologiques)* 53: 568–587.
- Habib E, Malakpet CG, Tokay A, et al. (2008b) Sensitivity of streamflow simulations to temporal variability and estimation of Z-R relationships. *Journal of Hydrologic Engineering* 13: 1177–1186.
- Hall DK, Riggs GA, Salomonson VV, et al. (2002) MODIS snow-cover products. *Remote Sensing of Environment* 83: 181–194.
- Han X and Li X (2008) An evaluation of the nonlinear/non-Gaussian filters for the sequential data assimilation. *Remote Sensing of Environment* 112: 1434–1449.
- He X, Vejen F, Stisen S, et al. (2011) An operational weather radar-based quantitative precipitation estimation and its

- application in catchment water resources modeling. *Soil Science Society of America* 10: 8–24.
- Houser PR, Shuttleworth WJ, Famiglietti JS, et al. (1998) Integration of soil moisture remote sensing and hydrologic modeling using data assimilation. *Water Resources Research* 34: 3405–3420.
- Huete A, Didan K, Miura T, et al. (2002) Overview of the radiometric and biophysical performance of the MODIS vegetation indices. *Remote Sensing of Environment* 83: 195–213.
- Huffman GJ, Adler RF, Bolvin DT, et al. (2007) The TRMM Multisatellite Precipitation Analysis (TMPA): Quasi-global, multiyear, combined sensor precipitation estimates at fine scales. *Journal of Hydrometeorology* 8: 38–55.
- Immerzeel WW and Droogers P (2008) Calibration of a distributed hydrological model based on satellite evapotranspiration. *Journal of Hydrology* 349: 411–424.
- Jackson TJ (1997) Soil moisture estimation using special satellite microwave/imager satellite data over a grassland region. *Water Resources Research* 33: 1475–1484.
- Jackson TJ (2005) Estimation of surface soil moisture using microwave sensors. *Encyclopedia of Hydrology* 54: 799–809.
- Jacobs JM, Meyers DA and Whitfield BM (2003) Improved rainfall/runoff estimates using remotely-sensed soil moisture. *Journal of the American Water Resources Association* 39: 313–324.
- Jiang L and Islam S (2001) Estimation of surface evaporation map over southern Great Plains using remote sensing data. *Water Resources Research* 37: 329–340.
- Joyce RJ, Janowiak JE, Arkin PA, et al. (2004) CMORPH: A method that produces global precipitation estimates from passive microwave and infrared data at high spatial and temporal resolution. *Journal of Hydrometeorology* 5: 487–503.
- Kalinga OA and Gan TY (2010) Estimation of rainfall from infrared-microwave satellite data for basin-scale hydrologic modelling. *Hydrological Processes* 24: 2068–2086.
- Kamble B and Irmak A (2008) Assimilating remote sensing-based ET into SWAP model for improved estimation of hydrological predictions. *IGARSS 2008 IEEE International Geoscience and Remote Sensing Symposium* 3: 1036–1039.
- Kelly R (2009) The AMSR-E snow depth algorithm: Description and initial results. *Journal of the Remote Sensing Society of Japan* 29: 307–317.
- Kelly RE, Chang AT, Tsang L, et al. (2003) A prototype AMSR-E global snow area and snow depth algorithm. *IEEE Transactions on Geoscience and Remote Sensing* 41: 230–242.
- Kerr YH, Waldteufel P, Richaume P, et al. (2012) The SMOS soil moisture retrieval algorithm. *IEEE Transactions on Geoscience and Remote Sensing* 50: 1384–1403.
- Kidder SQ and Vonder Haar TH (1995) *Satellite Meteorology: An Introduction*. San Diego, CA: Academic Press.
- Kite GW and Pietroniro A (1996) Remote sensing applications in hydrological modeling. *Hydrological Sciences Journal (Journal des Sciences Hydrologiques)* 41: 563–591.
- Kitzmler D, Van Cooten S, Ding F, et al. (2011) Evolving multisensor precipitation estimation methods: Their impacts on flow prediction using a distributed hydrologic model. *Journal of Hydrometeorology* 12: 1414–1431.
- Kolberg S, Rue H and Gottschalk L (2006) A Bayesian spatial assimilation scheme for snow coverage observations in a gridded snow model. *Hydrology and Earth System Sciences* 10: 369–381.
- Kongoli C, Dean CA, Helfrich SR, et al. (2007) Evaluating the potential of a blended passive microwave-interactive multi-sensor product for improved mapping of snow cover and estimations of snow water equivalent. *Hydrological Processes* 21: 1597–1607.
- Koster RD, Suarez MJ, Ducharme A, et al. (2000) A catchment-based approach to modeling land surface processes in a general circulation model: 1. Model structure. *Journal of Geophysical Research* 105: 24809–24822.
- Kuchment LS, Romanov P, Gelfan AN, et al. (2010) Use of satellite-derived data for characterization of snow cover and simulation of snowmelt runoff through a distributed physically based model of runoff generation. *Hydrology and Earth System Sciences* 14: 339–350.
- Kumar SV, Reichle RH, Harrison KW, et al. (2012) A comparison of methods for a priori bias correction in soil moisture data assimilation. *Water Resources Research* 48: W03515.
- Kummerow C, Olson W and Giglio K (1996) A simplified scheme for obtaining precipitation and vertical hydrometeor profiles from passive microwave sensors. *IEEE Transactions on Geoscience and Remote Sensing* 34: 1213–1232.

- Leuning R, Zhang Y, Rajaud A, et al. (2008) A simple surface conductance model to estimate evaporation using MODIS leaf area index and the Penman-Monteith equation. *Water Resources Research* 44: W10419.
- Li Z-L, Tang R, Wan Z, et al. (2009) A review of current methodologies for regional evapotranspiration estimation from remotely sensed data. *Sensors* 9: 3801–3853.
- Liang T, Zhang X, Xie H, et al. (2008) Toward improved daily snow cover mapping with advanced combination of MODIS and AMSR-E measurements. *Remote Sensing of Environment* 112: 3750–3761.
- Liston G and Hiemstra CA (2008) A simple data assimilation system for complex snow distributions (SnowAssim). *Journal of Hydrometeorology* 9: 989–1004.
- Liu T, Willems P, Feng XW, et al. (2012) On the usefulness of remote sensing input data for spatially distributed hydrological modeling: Case of the Tarim River basin in China. *Hydrological Processes* 26: 335–344.
- Liu Y and Gupta HV (2007) Uncertainty in hydrologic modeling: Toward an integrated data assimilation framework. *Water Resources Research* 43: W07401.
- Liu Y, Weerts AH, Clark M, et al. (2012) Advancing data assimilation in operational hydrologic forecasting: Progresses, challenges, and emerging opportunities. *Hydrology and Earth System Sciences* 16: 3863–3887.
- Loheide SP and Gorelick SM (2005) A local-scale, high-resolution evapotranspiration mapping algorithm (ETMA) with hydroecological applications at riparian meadow restoration sites. *Remote Sensing of Environment* 98: 182–200.
- Loumagne C, Normand M, Riffard M, et al. (2001) Integration of remote sensing data into hydrological models for reservoir management. *Hydrological Sciences Journal (Journal des Sciences Hydrologiques)* 46: 89–102.
- Makkink GF (1957) Testing the Penman formula by means of lysimeters. *Journal of the Institution of Water Engineers* 11: 277–288.
- Malakoff DM (1999) Bayes offers ‘new’ way to make sense of numbers. *Science* 286: 1460–1464.
- Manninen T, Stenberg P, Rautiainen M, et al. (2005) Leaf area index estimation of boreal forest using ENVISAT ASAR. *IEEE Transactions on Geoscience and Remote Sensing* 43: 2627–2635.
- Margulis SA, McLaughlin D, Entekhabi D, et al. (2002) Land data assimilation and estimation of soil moisture using measurements from the Southern Great Plains 1997 field experiment. *Water Resources Research* 38: 1299.
- Mattia F, Satalino G, Pauwels VRN, et al. (2009) Soil moisture retrieval through a merging of multi-temporal L-band SAR data and hydrologic modeling. *Hydrology and Earth System Sciences* 13: 343–356.
- Merlin O, Chehbouni A, Boulet G, et al. (2006) Assimilation of disaggregated microwave soil moisture into a hydrologic model using coarse-scale meteorological data. *Journal of Hydrometeorology* 7: 1308–1322.
- Merzouki A, McNairn H and Pacheco A (2011) Mapping soil moisture using RADARSAT-2 data and local autocorrelation statistics. *IEEE Journal of Selected Topics in Applied Earth Observations and Remote Sensing* 4: 128–137.
- Miller RN, Carter EF and Blue ST (1999) Data assimilation into nonlinear stochastic models. *Tellus Series A: Dynamic Meteorology and Oceanography* 51: 167–194.
- Moradkhani H (2008) Hydrologic remote sensing and land surface data assimilation. *Sensors* 8: 2986–3004.
- Moradkhani H, DeChant CM and Sorooshian S (2012) Evolution of ensemble data assimilation for uncertainty quantification using the particle filter-Markov chain Monte Carlo method. *Water Resources Research* 48: W12520.
- Moradkhani H, Hsu K, Hong Y, et al. (2006) Investigating the impact of remotely sensed precipitation and hydrologic model uncertainties on the ensemble streamflow forecasting. *Geophysical Research Letters* 33: L12107.
- Moradkhani H, Sorooshian S, Gupta HV, et al. (2005) Dual state-parameter estimation of hydrologic models using ensemble Kalman filter. *Advances in Water Resources* 28: 135–147.
- Morsdorf F, Kötz B, Meier E, et al. (2006) Estimation of LAI and fractional cover from small footprint airborne laser scanning data based on gap fraction. *Remote Sensing of Environment* 104: 50–61.
- Myneni RB, Hoffman S, Knyazikhin Y, et al. (2002) Global products of vegetation leaf area and fraction absorbed PAR from year one of MODIS data. *Remote Sensing of Environment* 83: 214–231.
- Ni-Meister W, Houser PR and Walker JP (2006) Soil moisture initialization for climate prediction: Assimilation of scanning multifrequency microwave radiometer soil moisture data into a land surface model.

- Journal of Geophysical Research: Atmospheres* 111: D20102.
- Njoku EG, Jackson TJ, Lakshmi V, et al. (2003) Soil moisture retrieval from AMSR-E. *IEEE Transactions on Geoscience and Remote Sensing* 41: 215–229.
- Painter TH, Rittger K, McKenzie C, et al. (2009) Retrieval of subpixel snow covered area, grain size, and albedo from MODIS. *Remote Sensing of Environment* 113: 868–879.
- Parajka J and Blöschl G (2008) The value of MODIS snow cover data in validating and calibrating conceptual hydrologic models. *Journal of Hydrology* 358: 240–258.
- Parajka J, Naemi V, Blöschl G, et al. (2009) Matching ERS scatterometer based soil moisture patterns with simulations of a conceptual dual layer hydrologic model over Austria. *Hydrology and Earth System Sciences* 13: 259–271.
- Parajka J, Naemi V, Blöschl G, et al. (2006) Assimilating scatterometer soil moisture data into conceptual hydrologic models at the regional scale. *Hydrology and Earth System Sciences* 10: 353–368.
- Pauwels VRN, Hoeben R, Verhoest NEC, et al. (2002) Improvements of TOPLATS-based discharge predictions through assimilation of ERS-based remotely-sensed soil moisture values. *Hydrological Processes* 16: 995–1013.
- Pereira-Cardenal SJ, Riegels ND, Berry PAM, et al. (2011) Real-time remote sensing driven river basin modeling using radar altimetry. *Hydrology and Earth System Sciences* 15: 241–254.
- Pham DT (2001) Stochastic methods for sequential data assimilation in strongly nonlinear systems. *Monthly Weather Review* 129: 1194–1207.
- Pomeroy JW, Gray DM, Brown T, et al. (2007) The Cold Regions Hydrological Model, a platform for basing process representation and model structure on physical evidence. *Hydrological Processes* 21: 2650–2667.
- Qin C, Jia Y, Su Z, et al. (2008) Integrating remote sensing information into a distributed hydrological model for improving water budget predictions in large-scale basins through data assimilation. *Sensors* 8: 4441–4465.
- Rango A (1994) Application of remote sensing methods to hydrology and water resources. *Hydrological Sciences Journal* 39: 309–320.
- Reichle RH (2008) Data assimilation methods in the Earth sciences. *Advances in Water Resources* 31: 1411–1418.
- Reichle RH and Koster RD (2004) Bias reduction in short records of satellite soil moisture. *Geophysical Research Letters* 31: L19501.
- Reichle RH and Koster RD (2005) Global assimilation of satellite surface soil moisture retrievals into the NASA Catchment land surface model. *Geophysical Research Letters* 32: L02404.
- Reichle RH, Entekhabi D and McLaughlin DB (2001a) Downscaling of radio brightness measurements for soil moisture estimation: A four-dimensional variational data assimilation approach. *Water Resources Research* 37: 2353–2364.
- Reichle RH, Koster RD, Dong J, et al. (2004) Global soil moisture from satellite observations, land surface models, and ground data: Implications for data assimilation. *Journal of Hydrometeorology* 5: 430–442.
- Reichle RH, Koster RD, Liu P, et al. (2007) Comparison and assimilation of global soil moisture retrievals from the Advanced Microwave Scanning Radiometer for the Earth Observing System (AMSR-E) and the Scanning Multichannel Microwave Radiometer (SMMR). *Journal of Geophysical Research* 112: D09108.
- Reichle RH, McLaughlin DB and Entekhabi D (2001b) Variational data assimilation of microwave radio brightness observations for land surface hydrology applications. *IEEE Transactions on Geoscience and Remote Sensing* 39: 1708–1718.
- Reichle RH, McLaughlin DB and Entekhabi D (2002) Hydrologic data assimilation with the ensemble Kalman filter. *Monthly Weather Review* 130: 103–114.
- Rodell M and Houser PR (2004) Updating a land surface model with MODIS-derived snow cover. *Journal of Hydrometeorology* 5: 1064–1075.
- Rodríguez E, Navascués B, Ayuso JJ, et al. (2003) Analysis of surface variables and parameterization of surface processes in HIRLAM. Part I: Approach and verification by parallel runs. HIRLAM Technical Report 58, 52 pp.
- Rosenthal W and Dozier J (1996) Automated mapping of montane snow cover at subpixel resolution from the Landsat Thematic Mapper. *Water Resources Research* 32: 115–130.
- Roy A, Royer A and Turcotte R (2010) Improvement of springtime streamflow simulations in a boreal environment by incorporating snow-covered area derived from remote sensing data. *Journal of Hydrology* 390: 35–44.

- Ryzhkov AV, Schuur TJ, Burgess DW, et al. (2005) The Joint Polarization Experiment. *Bulletin of the American Meteorological Society* 86: 809–824.
- Safari A and De Smedt F (2008) Streamflow simulation using radar-based precipitation applied to the Illinois River basin in Oklahoma, USA. Paper presented at the Third International Scientific Conference BALWOIS 2008: Water Observation and Information Systems for Decision Support, Ohrid, Republic of Macedonia, 27–31 May.
- Salvucci GD and Entekhabi D (2011) An alternate and robust approach to calibration for the estimation of land surface model parameters based on remotely sensed observations. *Geophysical Research Letters* 38: L16404.
- Seo D, Koren V and Cajina N (2003a) Real-time variational assimilation of hydrologic and hydrometeorological data into operational hydrologic forecasting. *Journal of Hydrometeorology* 4: 627–641.
- Seo D, Koren V and Cajina N (2003b) Real-time assimilation of radar-based precipitation data and streamflow observations into a distributed hydrological model. In: Tachikawa Y, Vieux BE and Georgakakos KP (eds) *Weather Radar Information and Distributed Hydrological Modelling*. IAHS Publication No. 282. Wallingford: IAHS, 138–142.
- Shu Y (2010) Integrating remote sensing and hydrological modeling for groundwater resources assessment and sustainable use in the North China Plain. PhD thesis, University of Copenhagen.
- Slater AG and Clark MP (2006) Snow data assimilation via an ensemble Kalman filter. *Journal of Hydrometeorology* 7: 478–493.
- Stephens GL and Kummerow CD (2007) The remote sensing of clouds and precipitation from space: A review. *Journal of the Atmospheric Sciences* 64: 3742–3765.
- Stisen S and Sandholt I (2010) Evaluation of remote-sensing-based rainfall products through predictive capability in hydrological runoff modeling. *Hydrological Processes* 24: 879–891.
- Stisen S, Jensen KH, Sandholt I, et al. (2008) A remote sensing driven distributed hydrological model of the Senegal River basin. *Journal of Hydrology* 354: 131–148.
- Su H, Yang Z-L, Dickinson RE, et al. (2010) Multisensor snow data assimilation at continental scale: The value of Gravity Recovery and Climate Experiment terrestrial water storage information. *Journal of Geophysical Research* 115: D10104.
- Su H, Yang Z-L, Niu G, et al. (2008) Enhancing the estimation of continental-scale snow water equivalent by assimilating MODIS snow cover with the ensemble Kalman filter. *Journal of Geophysical Research* 113: D08120.
- Su Z (2002) The Surface Energy Balance System (SEBS) for estimation of turbulent heat fluxes. *Hydrology and Earth System Sciences* 6: 85–99.
- Sun C, Walker JP and Houser PR (2004) A methodology for snow data assimilation in land surface model. *Journal of Geophysical Research* 109: D08108.
- Sun X, Mein RG, Keenan TD, et al. (2000) Flood estimation using radar and raingauge data. *Journal of Hydrology* 239: 4–18.
- Tang Q and Lettenmaier DP (2010) Use of satellite snow-cover data for streamflow prediction in the Feather River Basin, California. *International Journal of Remote Sensing* 31: 3745–3762.
- Tang Q, Gao H, Lu H, et al. (2009) Remote sensing: Hydrology. *Progress in Physical Geography* 33: 490–509.
- Tekeli AE, Akyurek Z, Sorman AA, et al. (2005) Using MODIS snow cover maps in modeling snowmelt runoff process in the eastern part of Turkey. *Remote Sensing of Environment* 97: 216–230.
- Tucker CJ, Pinzon JE, Brown ME, et al. (2005) An extended AVHRR 8-km NDVI dataset compatible with MODIS and SPOT vegetation NDVI data. *International Journal of Remote Sensing* 26: 4485–4498.
- van Leeuwen PJ and Evensen G (1996) Data assimilation and inverse methods in terms of a probabilistic formulation. *Monthly Weather Review* 124: 2898–2913.
- Vazifedoust M, van Dam JC, Bastiaanssen WGM, et al. (2009) Assimilation of satellite data into agrohydrological models to improve crop yield forecasts. *International Journal of Remote Sensing* 30: 2523–2545.
- Vereecken H, Huisman JA, Bogaen H, et al. (2008) On the value of soil moisture measurements in vadose zone hydrology: A review. *Water Resources Research* 44: W00D06.
- Versegly DL (2000) The Canadian Sand Surface Scheme (CLASS): Its history and future. *Atmosphere – Ocean* 38: 1–13.
- Verstraeten WW, Veroustraete F and Feyen J (2005) Estimating evapotranspiration of European forests

- from NOAA-imagery at satellite overpass time: Towards an operational processing chain for integrated optical and thermal sensor data products. *Remote Sensing of Environment* 96: 256–276.
- Wagner W, Verhoest NEC, Ludwig R, et al. (2009) Remote sensing in hydrological sciences. *Hydrology and Earth System Sciences* 13: 813–817.
- Walker JP and Houser PR (2001) A methodology for initializing soil moisture in a global climate model: Assimilation of near-surface soil moisture observations. *Journal of Geophysical Research* 106(D11): 11761–11774.
- Wang L and Qu JJ (2009) Satellite remote sensing applications for surface soil moisture monitoring: A review. *Frontiers of Earth Science in China* 3: 237–247.
- Xu X, Howard K and Zhang J (2008) An automated radar technique for the identification of tropical precipitation. *Journal of Hydrometeorology* 9: 885–902.
- Yang D, Koike T and Tanizawa H (2004) Application of a distributed hydrological model and weather radar observations for flood management in the upper Tone River of Japan. *Hydrological Processes* 18: 3119–3132.
- Yang X and Delsole T (2009) Using the ensemble Kalman filter to estimate multiplicative model parameters. *Tellus* 61A: 601–609.
- Zaitchik BF and Rodell M (2009) Forward-looking assimilation of MODIS-derived snow-covered area into a land surface model. *Journal of Hydrometeorology* 10: 130–148.
- Zhan X, Zheng W, Meng J, et al. (2012) Impact of SMOS soil moisture data assimilation on NCEP-GFS forecasts. EGU General Assembly 2012, 22–27 April, Vienna, p. 12724.
- Zhang J, Howard K, Langston C, et al. (2011) National Mosaic and multi-sensor QPE (NMQ) system: Description, results and future plans. *Bulletin of the American Meteorological Society* 92: 1321–1338.
- Zhang Y and Wegehenkel M (2006) Integration of MODIS data into a simple model for the spatial distributed simulation of soil water content and evapotranspiration. *Remote Sensing of Environment* 104: 393–408.
- Zhang YQ, Chiew FHS, Zhang L, et al. (2009) Use of remotely sensed actual evapotranspiration to improve rainfall-runoff modeling in Southeast Australia. *Journal of Hydrometeorology* 10: 969–980.
- Zhao H and Fernandes R (2009) Daily snow cover estimation from Advanced Very High Resolution Radiometer Polar Pathfinder data over Northern Hemisphere land surfaces during 1982–2004. *Journal of Geophysical Research* 114: D05113.
- Zheng G and Moskal LM (2009) Retrieving leaf area index (LAI) using remote sensing: Theories, methods and sensors. *Sensors* 9: 2719–2745.
- Zhou MC, Ishidaira H, Hapuarachchi HP, et al. (2006) Estimating potential evapotranspiration using Shuttleworth–Wallace model and NOAA-AVHRR NDVI data to feed a distributed hydrological model over the Mekong River basin. *Journal of Hydrology* 327: 151–173.
- Zhou S, Liang X, Chen J, et al. (2004) An assessment of the VIC-3 L hydrological model for the Yangtze River basin based on remote sensing: A case study of the Baohe River basin. *Canadian Journal of Remote Sensing* 30: 840–853.